

## **Miocene evolution of the western edge of the Nevadaplano in the central and northern Sierra Nevada: palaeocanyons, magmatism, and structure**

Cathy J. Busby<sup>a\*</sup> and Keith Putirka<sup>b</sup>

<sup>a</sup>*Department of Earth Science, University of California, Santa Barbara, CA 93106, USA;*

<sup>b</sup>*Department of Earth and Environmental Sciences, California State University-Fresno, 2345 San Ramon Ave., MS/MH24, Fresno, CA 93720, USA*

(Accepted 17 April 2009)

The Sierra Nevada of California is the longest and tallest mountain range in the co-terminus USA, and has long been regarded as topographically very young (< 6 Ma); however, recent work has provided evidence that the range is very old (> 80 Ma), and represents the western shoulder of a Tibetan-like plateau (the Nevadaplano) that was centred over Nevada. A great deal of effort has been invested in applying modern laboratory and geophysical techniques to understanding the Sierra Nevada, yet some of the most unambiguous constraints on the Sierran landscape evolution are derived from field studies of dated strata preserved in the palaeochannels/palaeocanyons that crossed the range in Cenozoic time. Our work in the Sierra Nevada suggests that neither end-member model is correct for the debate regarding youth vs. antiquity of the range. Many features of the Cenozoic palaeocanyons and palaeochannels reflect the shape of the Cretaceous orogen, but they were also affected by Miocene tectonic and magmatic events. In the central Sierra Nevada, we infer that the inherited Cretaceous landscape was modified by three Miocene tectonic events, each followed by ~ 2–5 Myr of subduction-induced magmatism and sedimentation during a period of relative tectonic quiescence. The first event, at about 16 Ma, corresponds to the westward sweep of the Ancestral Cascades arc front into the Sierra Nevada and adjacent western Nevada. We suggest that this caused thermal uplift and extension. The second event, at about 11–10 Ma, records the birth of the ‘future plate boundary’ by transtensional faulting and voluminous high-K volcanism at the western edge of the Walker Lane belt. The third event, at about 8–7 Ma, is associated with renewed range-front faulting in the central Sierra, and rejuvenation and beheading of the palaeocanyons. Volcanic pulses closely followed all three events, and we tentatively infer that footwall uplift of the Sierra Nevada occurred during all three events. By analogy with the ~ 11 Ma event, we speculate that high-K volcanic rocks in the southern part of the range mark the inception of yet a fourth pulse of range-front faulting at 3–3.5 Ma, which resulted in a fourth tilting and crestal uplift event. Cenozoic rocks along the western edge of the Nevadaplano record the following variation, from the central to the northern Sierra: decrease in crustal thickness (and presumably palaeoelevation), decrease in palaeorelief and attendant decrease in coarse-grained fluvial- and mass-wasting deposits, and greater degree of encroachment by Walker Lane-related faults beginning at 10–11 Ma. By mapping and dating Cenozoic strata in detail, we show that what is now the Sierra Nevada was, at least in part, shaped by the Miocene structural and magmatic events.

**Keywords:** Sierra Nevada; Cascades arc; Walker Lane belt

---

\*Corresponding author. Email: [cathy@crustal.ucsb.edu](mailto:cathy@crustal.ucsb.edu)

## Introduction

Great controversy abounds regarding the age and uplift history of the longest and tallest mountain chain in the co-terminus USA. The Sierra Nevada (Figure 1) has long been considered one of the youngest ranges in North America (< 3–6 Ma), formed through an uplift of a rigid block about faults along its eastern margin (Whitney 1880; Lindgren 1911; Bateman and Wahrhaftig 1966; Hamilton and Myers 1966; Huber 1981; Ransome 1898;

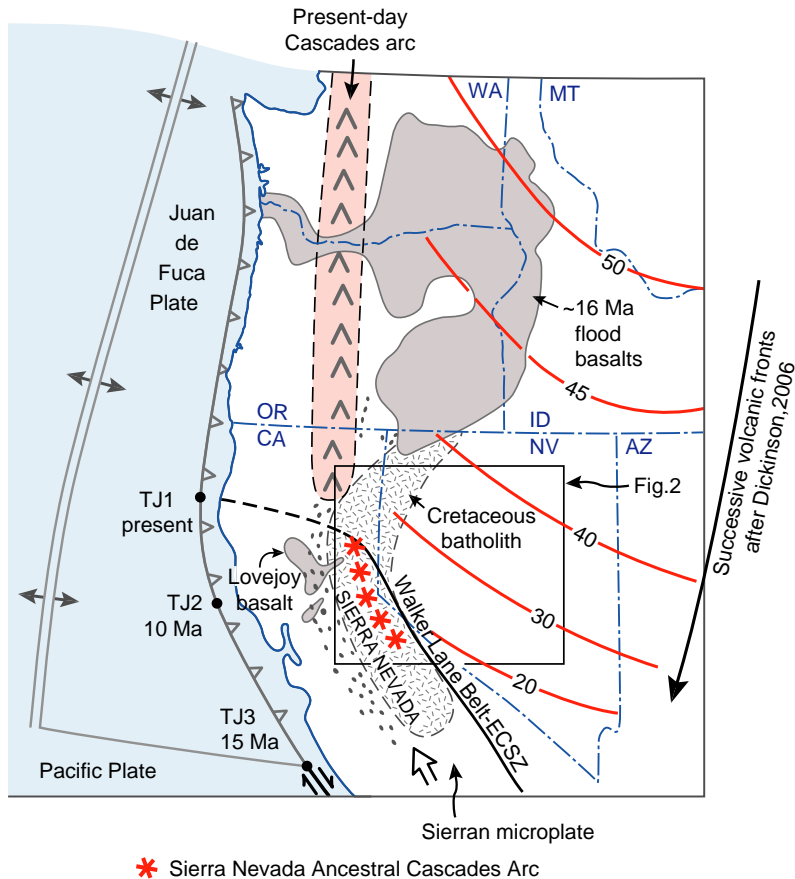


Figure 1. Tectonic setting of the Sierra Nevada. Shown are the locus of the Cretaceous Sierra Nevada batholith and its extension into northwest Nevada, and relicts of the basins active during unroofing of the batholith in Late Cretaceous-to-Tertiary time (dot pattern). Positions of the subduction-related magmatism in Cenozoic time are consistent with sea-floor evidence for subduction off California in Eocene-and-Oligocene time as summarized by Dickinson (2006) who interpreted the SSW-migrating magmatism to represent well-defined arc fronts that followed slab rollback. Sea-floor reconstruction at 15 Ma (Dickinson 1997), showing positions of the triple junction at 10 Ma and present. TJ1 marks the present position of the triple junction between the San Andreas fault, the Cascadia subduction zone, and the Mendocino fracture zone. The Sierran microplate lies between the San Andreas fault and the Walker Lane belt, which currently accommodates 20–25% of the plate motion between the North American and Pacific plates (see references in text), and may represent the future plate boundary. This was born at 11 Ma within the Sierra Nevada Ancestral Cascades arc (Putirka and Busby 2007) during high-K eruptions at the Little Walker Caldera (L.W., Figure 2).

Unruh 1991; Wakabayashi *et al.* 2001). More recent papers have proposed a more complex uplift history for the range, and some have argued for the antiquity of the range (>80 Ma; Wolfe *et al.* 1997; House *et al.* 1998, 2001; Horton *et al.* 2004; Stock *et al.* 2004; Clark *et al.* 2005; Cecil *et al.* 2006; Mulch *et al.* 2006). Evidence for significant late Cenozoic surface uplift includes tilting of Tertiary sedimentary units and river incision patterns (Christensen 1966; Huber 1981; Unruh 1991; Wakabayashi and Sawyer 2001; Jones *et al.* 2004). However, recent studies have mainly used laboratory techniques to infer that the range has been a long-standing topographic feature of the landscape in the western USA, including stable isotope studies (Poage and Chamberlain 2002; Horton *et al.* 2004; Horton and Chamberlain 2006; Mulch *et al.* 2006); thermochronology (House *et al.* 1998, 2001; Clark *et al.* 2005; Cecil *et al.* 2006; Mahéo *et al.* 2009); cosmogenic nuclide studies (Stock *et al.* 2005); palaeobotanical studies (Wolfe *et al.* 1997); dating of cave sediments (Stock *et al.* 2004); and hydrogen isotope studies of widespread ash-fall deposits (Mulch *et al.* 2008). Some workers, however, have proposed a more intermediate model, wherein a Cretaceous–Eocene inherited landscape surface began to undergo erosional rejuvenation sometime after 20 Ma (Clark *et al.* 2005; Clark and Farley 2007; Pelletier 2007), in response to the inception of the Sierra Nevada microplate (Mahéo *et al.* 2009; Saleeby *et al.* 2009). It is also clear that, in the southern Sierra, a phase of accelerated river incision began at ca. 3 Ma, in response to a > 1 km crestal uplift driven by the underlying mantle lithosphere foundering (Ducea and Saleeby 1996, 1998; Jones *et al.* 2004; Saleeby and Foster 2004; Zandt *et al.* 2004; Saleeby *et al.* 2009).

In this paper, we interpret new field and geochronological results gathered by us and our students over the past five years, on Cenozoic strata and intrusions in the central and northern Sierra Nevada (Figures 2–7; Table 1; Rouillet 2006; Busby *et al.* 2008a,b; Garrison *et al.* 2008; Gorny *et al.* 2009; Hagan *et al.* 2009; Koerner *et al.* 2009). These results provide a sensitive record of the surface processes over the past ~50 Myr, including:

- (1) Canyons and channels cut by ancient rivers whose lengths, gradients, and sedimentological characteristics were controlled by regional-scale elevation and topographic relief.
- (2) Evidence for long (ca. 2–10 Myr) periods of steady volcano-sedimentary aggradation that alternated with shorter periods of erosion and development of regional-scale unconformities.
- (3) An array of volcanic centre types, with distinctive eruptive styles, reflecting regional variation in lithospheric thickness, extensional vs. transtensional styles of faulting, and hot spot vs. subduction vs. continental rift magmatism.
- (4) Miocene episodes of faulting along the present-day range front and adjacent parts of Nevada to the east, recognized through detailed mapping of the dateable volcanic strata. These episodes appear to be synchronous with development of unconformities.

We offer a new model for the Cenozoic history of the central Sierra Nevada, where channels/canyons that were carved during the Cretaceous-to-Palaeocene uplift (referred to here as unconformity 1) were re-incised three times during the Miocene (unconformities 2–4), each in response to a tectonic event that immediately preceded a major pulse of magmatism (Figure 7). We present arguments for a fundamentally tectonic control on the development of the Miocene unconformities.

Another controversy related to the timing of the uplift of the Sierra Nevada is the circumstances surrounding the birth of the future plate boundary, which extends from the Gulf of California northwards through the Eastern California Shear Zone–Walker

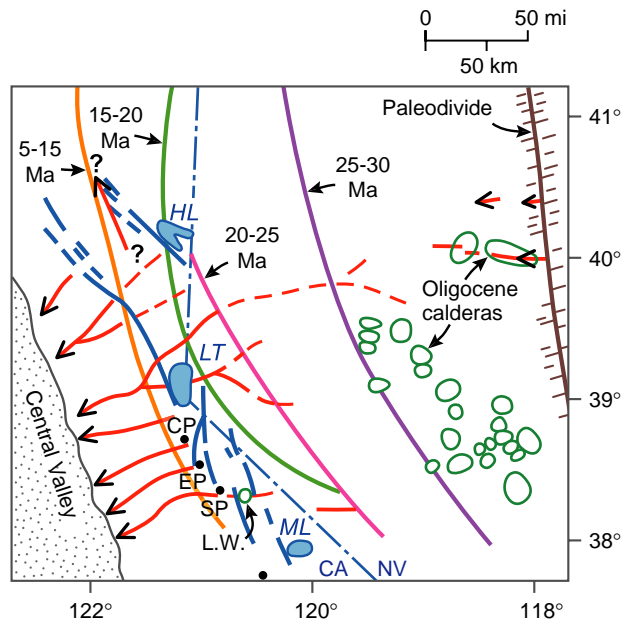


Figure 2. Oligocene-to-Miocene palaeogeography of part of the Basin and Range and Sierra Nevada, showing the position of the palaeodivide and Oligocene-to-early-Miocene calderas (Henry 2008), and Tertiary palaeochannels that funnelled ignimbrites westwards from the calderas in the central Nevada to the Central Valley of California (Henry 2008). The present-day Sierra Nevada range-front faults are shown in blue. Note that the palaeochannels are much better defined in the Sierra Nevada of California than they are in Nevada because they were not overprinted by prolonged subduction volcanism, nor were they disrupted by the Basin and Range faults; this makes them ideal for reconstruction of the landscape evolution. Progressive west-southwestward sweep of the Oligocene-to-Miocene arc front is shown, using the data summarized by Cousens *et al.* (2008) and our new dates (Figure 4). HL, Honey Lake; LT, Lake Tahoe; CP, Carson Pass; EP, Ebbetts Pass; SP, Sonora Pass; L.W., 11–9 Ma Little Walker Caldera; ML, Mono Lake.

Lane belt (Figure 1). This fault zone forms the transtensional eastern boundary between the Sierra Nevada microplate and the Basin and Range to the east (Figure 5; Argus and Gordon 1991; Dixon *et al.* 2000; Sella *et al.* 2002), and currently accommodates 20–25% of the plate motion between the Pacific and North American plates (Bennett *et al.* 1999; Thatcher *et al.* 1999; Dixon *et al.* 2000; Oldow 2000; Unruh *et al.* 2003). Recent field and geochronological studies in the Sierra Nevada have shown that this process began at 11 Ma, with the outpouring of voluminous, geochemically distinctive volcanic rocks, preceded by range-front transtensional faulting and probable uplift (Busby *et al.* 2008b).

### Old vs. young mountain range: magmatic and tectonic events

The long-accepted model for the origin of the Sierra Nevada involves an uplift of the range through tilting of a block bounded on the east by the westernmost and youngest fault zone of the Basin and Range extensional province, less than 6 Myr ago (Hamilton and Myers 1966; Figure 3). By contrast, recent papers have proposed that the Sierra Nevada formed along the western shoulder of a high, Tibetan-style plateau centred over Nevada about 80 Myr ago, and that the extension has caused Cenozoic basins to drop down from high

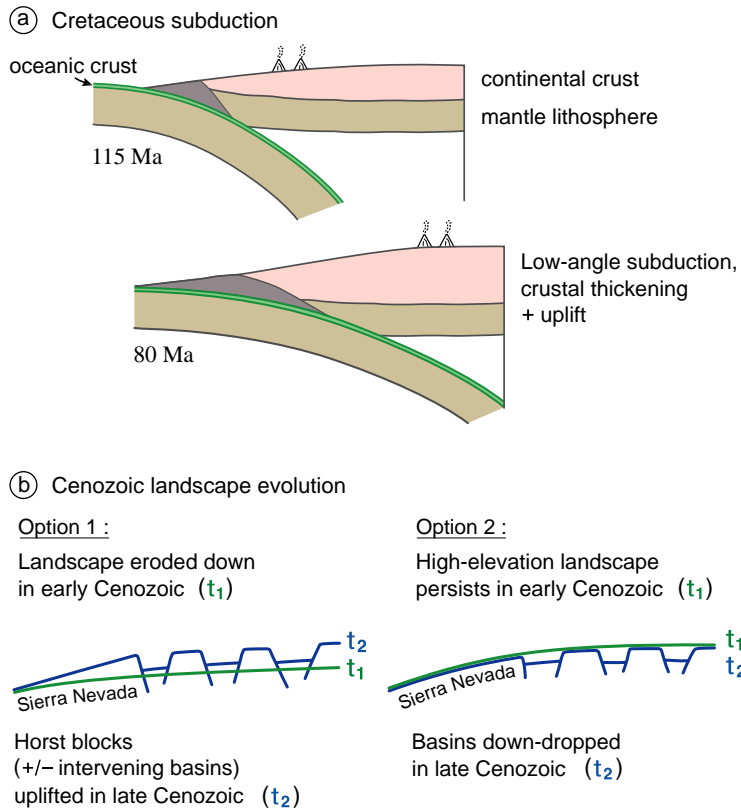


Figure 3. (a) Simplified cross-sectional view of the low-angle subduction that created a high plateau across Nevada and eastern California in Cretaceous time, referred to as the Nevadaplano (not drawn to scale) (DeCelles 2004). (b) A simple cartoon illustrating the end-member models for Cenozoic-landscape evolution (not to scale). Option 1: block-faulting model for uplift of the Sierra Nevada at 3–6 Ma (Hamilton and Myers 1966). Option 2: origin of the Sierra Nevada on the shoulder of a high plateau inherited from Cretaceous time, disrupted by down-dropping of basins in Cenozoic time.

elevations, with the Sierra Nevada and other ranges forming relict highs that have not been uplifted significantly in the Cenozoic (House *et al.* 1998; Figure 3). It is generally agreed that this high plateau or broad altiplano was formed by shortening and crustal thickening

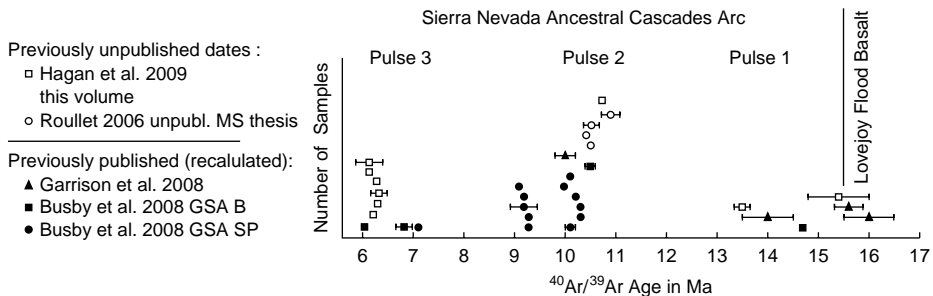


Figure 4. Distribution of our new  $^{40}\text{Ar}/^{39}\text{Ar}$  dates on previously undated rocks of the Sierra Nevada Ancestral Cascades arc.

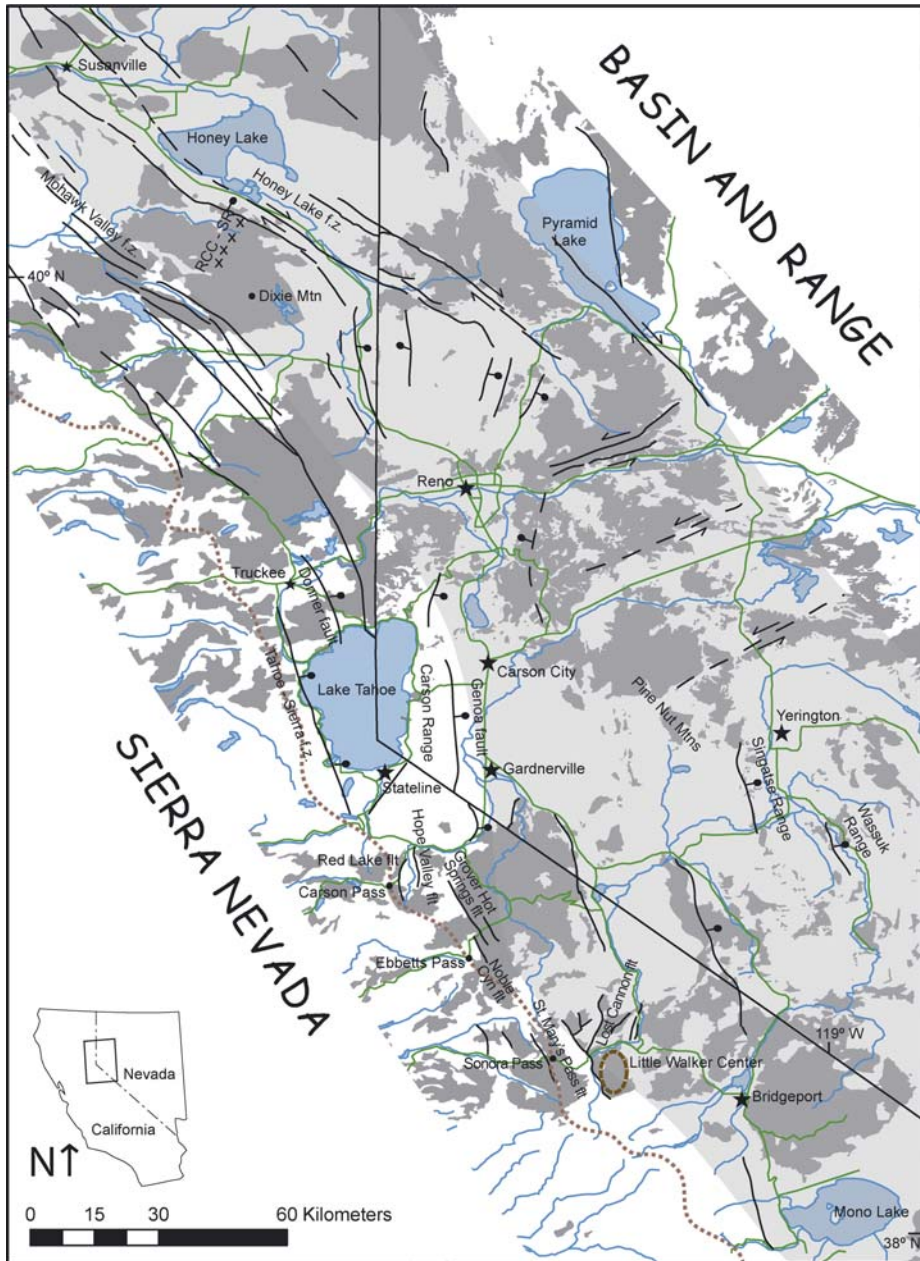


Figure 5. Distribution of Cenozoic volcanic rocks (dark grey) and faults along the central to northern Sierra Nevada–Basin and Range transition, with the area shaded in light grey representing the Walker Lane belt. The brown dotted line represents the present-day Sierra Nevada range crest. The brown circle represents the Little Walker Center/Caldera, described in the text. Sources include Koenig (1963), Stewart and Carlson (1978), Wagner *et al.* (1981), Saucedo and Wagner (1992), Henry and Perkins (2001), Saucedo (2005), Busby *et al.* (2008a,b), Hagan *et al.* (2009), and Cashman *et al.* (2009). RCC-SR, Red Clover Creek–Stony Ridge sections of Garrison *et al.* (2008).

due to Cretaceous low-angle subduction beneath the continental margin (DeCelles 2004; Figure 3(a)). There is a general agreement that during Cretaceous-to-Palaeocene time, the Cretaceous arc was unroofed to batholithic levels (Cecil *et al.* 2007) and 'palaeochannels' or 'palaeocanyons' were carved into it, and filled with Eocene-to-Miocene strata (Ransome 1898; Lindgren 1911; Bateman and Wahrhaftig 1966; Garside *et al.* 2005; Busby *et al.* 2008a,b).

The timing and cause of subsequent Cenozoic extension of this plateau remains controversial. Some workers infer that extension accompanied the southwestward sweep of arc magmatism as the subducting slab fell back to steeper depths during Eocene-to-Miocene time (Gans *et al.* 1989; Axen *et al.* 1993; Figure 1). Stable isotope studies on palaeosol carbonates, authigenic minerals, and metamorphic minerals in the normal faults have been used to infer that this southward sweep of arc magmatism and extension was accompanied by an increase in surface elevation, in places estimated at 2.5–3.5 km; this is consistent with models for thermal reorganization of the crust and lithosphere during removal of the Farallon slab or delamination of the mantle lithosphere (Horton and Chamberlain 2006; Kent-Corson *et al.* 2006; Mulch *et al.* 2007).

Our new age and geochemical data on 16–6 Ma subduction-related volcanic rocks in the central and northern Sierra, compiled here (Table 1), are consistent with Dickinson's (2007) reconstructions for the westward sweep of the arc into that region and coeval subduction off California (Sierra Nevada Ancestral Cascades arc, Figure 1; Putirka and Busby 2007; Busby *et al.* 2008b). We attribute the scarcity of subduction-related volcanic rocks and intrusions in the southern Sierra to a southward increase in thickness of the crust that underlays the Sierra Nevada Ancestral Cascades arc, and not to a lack of subduction at that latitude (Putirka and Busby 2007). We suggest below that uplift and extension not only accompanied southwestward sweep of magmatism through Basin and Range, but also accompanied emplacement of arc magmatic rocks in the Sierra Nevada.

We also summarize here data that demonstrate disruption of the western edge of the Nevadaplano as it began to calve off onto the Sierra Nevada microplate. As discussed by Saleeby *et al.* (2009), the eastern Sierran escarpment system and the Garlock transform fault serve as reasonable approximations to classic plate boundaries, while the western and northern boundaries of the microplate are highly diffuse transpressional and compressional boundaries (respectively) that are unlikely to yield definitive structural evidence for the timing of microplate inception. The data summarized here support the interpretation that this process began at 11 Ma.

This paper is not intended as a review of all previous laboratory-based work on the landscape evolution of the Sierra Nevada; instead, it focuses on the stratigraphic record of the palaeochannels/palaeochannel fills, as well as age patterns of associated intrusions, and attempts to reconcile these data with seemingly contradictory laboratory and seismic data. This paper does not discuss the Cenozoic evolution of the southern Sierra Nevada, partly because palaeocanyons have not been resolved there (Saleeby *et al.* 2009), but largely because that segment has a Cenozoic history that is distinctly different from the rest of the Sierra Nevada; for a full discussion with references, see Saleeby *et al.* (2009, this volume). This paper presents a new reconstruction of the evolution of the central-to-northern Sierra Nevada (Figure 7), using Cenozoic volcanic and volcanoclastic strata that are largely preserved in the palaeochannels (Figure 2). We then interpret these palaeochannels in the larger context of Cretaceous-to-Cenozoic landscape evolution of the western USA.

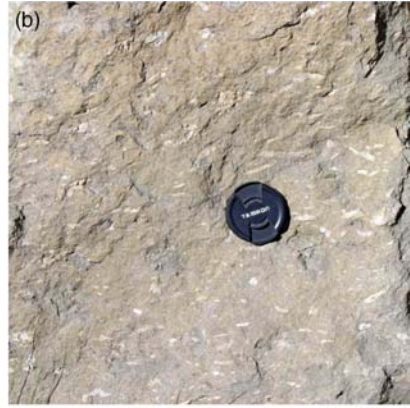
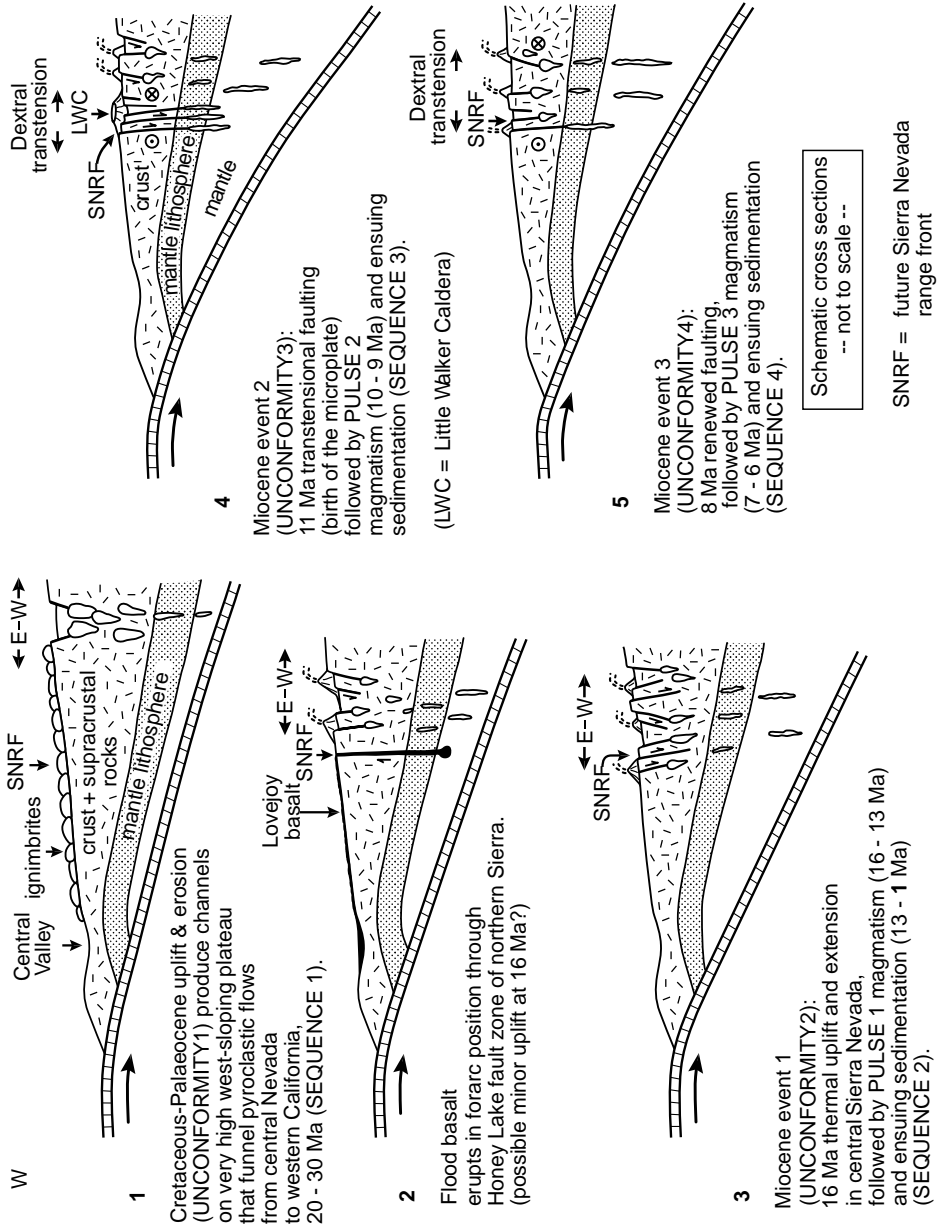






Figure 6. Outcrop photos of the selected key features in the Sierra Nevada palaeocanyons. (a) Unconformity 1, showing the rugged palaeorelief carved into the Mesozoic mesozonal granitic rock below; Tertiary volcanic–volcaniclastic rocks above. Photo taken on the southeast side of Stanislaus Peak. (b) Sequence 1 weakly welded Oligocene ignimbrite, erupted from the central Nevada; note the small size of flattened pumices, which is typical of these distal ignimbrites. (c) Unconformity 2, cut into sequence 1 Oligocene ignimbrites (not visible in photo) and overlain by Miocene andesitic volcaniclastic rocks with a basal lag of well-rounded granitic cobbles and boulders. Granitic clasts are very rare in the Miocene volcanic–volcaniclastic section, except along the unconformities. (d) Sequence 2 avalanche blocks composed of block-and-ash-flow tuff (yellow), enclosed in debris flow deposits at Carson Spur (map unit Tfdf, interstratified fluvial and debris flow deposits, Figure 2 of Busby *et al.* (2008a)). The avalanche blocks were derived from a 15 Ma hornblende trachyandesite block-and-ash-flow tuff preserved at the modern Sierran crest, 8 km up-palaeocanyon (Thabal of Hagan *et al.* (2009)). (e) Petrified wood is common in the debris flow deposits, and charred wood occurs in the block-and-ash-flow tuffs of the palaeocanyon fills; this example is from sequence 2. (f) Andesite block-and-ash-flow tuff, typical of sequences 2–4: they are massive, with monomict angular-to-subrounded blocks up to 1 m in diameter, set in an unsorted lapilli- to ash-sized matrix of the same composition. This photo comes from sequence 2 at Sonora Pass (Relief Peak Formation). (g) Interstratified andesitic debris flow and fluvial deposits, typical of sequences 2–4. Debris flow deposits are massive, unsorted, and contain a variety of andesite clast types supported in a pebbly sandstone matrix, whereas the fluvial deposits are stratified and sorted, and show better rounding of clasts. These strata are tilted because they lie within a 1.6 km-long avalanche block derived from sequence 2 by landsliding along a range-front fault immediately prior to the eruption of sequence 3 high-K rocks at the Sonora Pass. (h) Fluvial boulder conglomerate typical of sequences 2–4. Note imbrication. (i) Fluvial pebble and cobble conglomerate typical of sequences 2–4. (j) Angular unconformity (unconformity 3) produced by the sliding of megablocks of sequence 2 strata onto the downthrown block of a range-front fault (tilted strata), within 140 kyr of the eruption of the overlying sequence 3 Table Mountain Latite lava flows from the Little Walker Center (overlying flat-lying strata). Unconformity 3, elsewhere, consists of an erosional unconformity (see text). Photo taken on the east side of the Sonora Pass, looking south towards Sardine Falls (lower left). (k) Sequence 3 high-K lava flows of the Table Mountain Latite: trachyandesite and trachybasaltic andesite. In this flow, the columnar-jointed base passes upwards into complexly blocky-jointed top typical of lava quenched by water running over it. This is consistent with its emplacement in a palaeoriver canyon. Photo taken west of Sonora Pass in the Dardanelles area. (l) Stretched vesicles in the Table Mountain Latite, oriented parallel to the WSW–ENE-trending palaeocanyon (Koerner *et al.* 2009). (m) Sequence 3 high-K ignimbrite of the Eureka Valley Tuff: trachydacite (Koerner *et al.* 2009). This outcrop passes upwards from glassy, densely welded ignimbrite into devitrified, less densely welded ignimbrite. (n) A close-up of the Eureka Valley Tuff (sequence 3), showing typical black fiamme, and abundant light grey volcanic rock fragments. (o) A conglomerate overlying unconformity 4: Megaboulders of the granitic basement encased in a cobble to boulder conglomerate with andesitic and granitic clasts. These clasts were funnelled down a relay ramp between overlapping normal faults (see text). (p) Sequence 4 breccias, Ebbetts Pass: extremely coarse-grained deposits record rejuvenation and beheading of the palaeocanyon system along range-front faults at about 7 Ma. (q) Sequence 4 basalt lava flow, showing a well-developed a'a crust; other basalt flows in the section have pahoehoe crusts, but andesite block-and-ash-flow tuffs and lava flows dominate sequence 4 (Hagan *et al.* 2009). (r) Sequence 4 Ebbetts Pass Center, sited on the Grover Hot Spring fault (not visible): The strata on the right side of the photo consist of basaltic andesite lava flows that dip away from the centre, with a primary dip angle of about 30°. Light grey rocks on the skyline at the left side of the photo are dacite intrusions that form the core of the centre. Our unpublished mapping shows that basaltic andesite lava flows dip away from the silicic intrusive core to form a mafic shield with a radius of about 8 km. Field view of the photo is about 4 km.



### Palaeochannels, faults and Ancestral Cascades arc volcanism, central and northern Sierra Nevada

Palaeochannels of the Sierra Nevada generally trend E–W (Figure 2) and the material in them was transported from east to west, as in the modern drainages (Whitney 1880; Ransome 1898; Lindgren 1911; Bateman and Wahrhaftig 1966; Wakabayashi and Sawyer 2001; Garside *et al.* 2005; Busby *et al.* 2008a,b; Henry 2008). These palaeochannels are much better preserved and exposed in the Sierra Nevada than they are in the Basin and Range to the east (Figure 2), due to disruption by faults and burial beneath the basins there. Thus, Sierran palaeochannels provide the best opportunity to understand the palaeogeography of the western flank of the ‘Nevadaplano’ (DeCelles 2004).

In this paper, we synthesize newly published mapping and  $^{40}\text{Ar}/^{39}\text{Ar}$  dating of the palaeochannel fill in the northern and central Sierra Nevada (Busby *et al.* 2008a,b; Garrison *et al.* 2008; Hagan *et al.* 2009; Koerner *et al.* 2009; Figure 4) to define these magmatic and inferred tectonic events (Figure 7):  $\sim 16$  Ma flood basalt volcanism and weak extension in the northern Sierra, and three distinct episodes of Miocene faulting and possible uplift in the central Sierra, at about 16, 11, and 8–7 Ma. Each of the three postulated Miocene uplift events is recognized by an erosional unconformity that has been mapped out along the axes of the palaeocanyons, and correlates between the palaeocanyons of the central Sierra (Busby *et al.* 2008a,b; Hagan *et al.* 2009). We refer to the unconformity between the granitic bedrock and the Oligocene ignimbrites as unconformity 1, and the three Miocene unconformities as unconformities 2–4 (Figure 7; Hagan *et al.* 2009). Minor erosional surfaces locally occur between these unconformities but these cannot be traced out for any distance. For example, two unconformities in the modern Kirkwood Valley (unconformities 4 and 5 of Busby *et al.* 2008a) could not be correlated to the other palaeocanyons (Busby *et al.* 2008a,b), and are now known to merge with up-palaeocanyon with unconformity 3 of this paper (Hagan *et al.* 2009). Each of the three inferred Miocene uplift events was separated by longer periods of aggradation of arc volcanic and sedimentary rocks, with no evidence of re-incision in the palaeocanyons (Figure 7). This aggradation produced unconformity-bounded sequences, which are given the number of the unconformity that underlies them, as is customary (see references in Busby and Bassett 2007). Thus, in the central Sierra, sequence 1 consists of the basal Oligocene ignimbrites, which rest upon the granitic basement. Sequences 2, 3, and 4 consists of Miocene volcanic and volcanoclastic rocks that are  $\sim 16$ –11 Ma (middle Miocene),  $\sim 10$ –8 Ma (early late Miocene), and 7–6 Ma (late late Miocene) in age, respectively. Work in progress will more closely define the ages of unconformities and sequences.

In this section, we use a time-slice approach to describe and interpret key features of the mapped and dated unconformities and sequences. We also describe any direct or indirect links we can make between the development of unconformities and faulting in the region. In the following section, we discuss possible alternative explanations for the development of the unconformities (e.g. changes in climate, sediment supply, etc.) and explain why we prefer a tectonic explanation for their origin.



Figure 7. Sketch model for the Cenozoic tectonic evolution of the central Sierra Nevada. The cartoon cross-sections illustrate key features in the crust and subducting slab, and are not drawn to scale.

Table 1. Summary of our <sup>40</sup>Ar/<sup>39</sup>Ar age data on the Cenozoic volcanic rocks in the central and northern Sierra Nevada.

Sample no.	Geochem	Mineral	Lat (°N)	Long (°W)	Interpreted age (Ma) <sup>a</sup>		Nominal age (Ma) <sup>b</sup>		Preferred age (Ma) <sup>c</sup>		Unit name	
					Age	±2s	Age	±2s	Age	±2s		
(A) Sonora Pass (Busby <i>et al.</i> 2008b)												
BP068	Andesite	Hbl	38.37609	119.76975	7.12	0.06	7.22	0.06	7.28	0.06	Hbl Andesite Plug – Disaster Peak Fm	
BP068	Andesite	Plag	38.37609	119.76975	7.0	0.5	7.11	0.5	7.15	0.5	Hbl Andesite Plug – Disaster Peak Fm	
TF003	Trachydacite	Plag	38.43096	119.44792	9.14	0.04	9.28	0.04	9.34	0.04	Upper Member, Eureka Valley Tuff – Stanislaus Gp	
TF003	Trachydacite	Bio	38.43096	119.44793	9.18	0.04	9.32	0.04	9.38	0.04	Upper Member, Eureka Valley Tuff – Stanislaus Gp	
TF005b	Trachydacite	Plag	38.43041	119.44805	9.2	0.3	9.34	0.3	9.4	0.3	By-Day Member, Eureka Valley Tuff – Stanislaus Gp	
TF009	Trachydacite	Plag	38.42891	119.44841	9.27	0.04	9.41	0.04	9.47	0.04	Tollhouse Flat Member, Eureka Valley Tuff – Stanislaus Gp	
TF009	Trachydacite	Bio	38.42891	119.44842	9.34	0.04	9.48	0.04	9.54	0.04	Tollhouse Flat Member, Eureka Valley Tuff – Stanislaus Gp	
PC032	Shoshonite	Plag	38.35378	119.6344	10.14	0.06	10.30	0.06	10.36	0.06	Uppermost Table Mtn Latite Flow – Stanislaus Gp	
PC005	Trachyandesite	Plag	38.34641	119.63263	10.19	0.08	10.35	0.08	10.41	0.08	Lowermost Table Mtn Latite Flow – Stanislaus Gp	
PC-AD	Andesite	WR	38.34641	119.63265	10.35	0.25	10.51	0.25	10.58	0.25	Andesite dike – Upper Relief Peak Fm	

Table 1 – continued

Sample no.	Geochem	Mineral	Lat (°N)	Long (°W)	Interpreted age (Ma) <sup>a</sup>		Nominal age (Ma) <sup>b</sup>		Preferred age (Ma) <sup>c</sup>		Unit name	Map unit
					Age	±2s	Age	±2s	Age	±2s		
PC-BA	Basaltic andesite	Hbl	38.34427	119.6340	10.17	0.18	10.33	0.18	10.39	0.18	Block-and-ash flow tuff	
PC-BA	Basaltic andesite	Plag	38.34427	119.6341	~10	na	~10	na	~10	na	– Upper Relief Peak Fm Block-and-ash flow tuff	
BP057	–	Plag	38.37824	119.7430	23.8	0.2	24.16	0.2	24.32	0.2	– Upper Relief Peak Fm Uppermost welded ignimbrite – Valley Springs Fm	
(B) Carson Pass–Kirkwood (Busby <i>et al.</i> 2008a)												
SBDCP61	Andesite	Plag	38.6979	120.0888	6.05	0.12	6.14	0.12	6.18	0.12	Sentinels block-and-ash-flow tuff	Taba3
SBDCP62	Basalt	WR	38.7101	120.0187	6.80	0.20	6.90	0.20	6.95	0.20	Basalt lava flow	Tbl
SBDCP20	Andesite	Plag	38.6855	120.0617	10.49	0.12	10.65	0.12	10.72	0.12	Peperitic andesite dike in debris flow deposit	Tvdf1
SBDCP30	Trachyandesite	Bio	38.7014	120.0003	14.69	0.06	14.91	0.06	15.01	0.06	Carson Pass hornblende trachyandesite block-and-ash-flow tuff	Thaba1
(C) Hope Valley–Carson Pass (Hagan <i>et al.</i> 2009)												
ERLPk	Basaltic andesite	Hbl	38.7158	119.9857	na		6.09	0.34	6.13	0.34	Red Lake Pk pyroxene basaltic andesite block-and-ash-flow tuff	Tpaba
JHCP-67	Andesite	Hbl	38.6600	119.8996	na		6.14	0.14	6.18	0.14	Markleeville Pk hb-bt dacite and andesite intrusions	Thbdi
JHCP-56	Andesite	Hbl	38.6909	119.9799	na		6.18	0.14	6.22	0.14	Lower hornblende andesite lava flow	Thalu
JHCP-13	Basaltic andesite	Hbl	38.7122	119.9856	na		6.25	0.10	6.29	0.10	Red Lake Pk pyroxene basaltic andesite block-and-ash-flow tuff	Tpaba

Table 1 – continued

Sample no.	Geochem	Mineral	Lat (°N)	Long (°W)	Interpreted age (Ma) <sup>a</sup>		Nominal age (Ma) <sup>b</sup>		Preferred age (Ma) <sup>c</sup>		Unit name	Map unit
					Age	±2s	Age	±2s	Age	±2s		
JHCP-53	Dacite	Hbl	38.6581	119.9233	na		6.30	0.14	6.34	0.14	Markleeville Pk hb-bt dacite and andesite intrusions	Thbdi
JHCP-69	Andesite	Hbl	38.6644	119.8947	na		6.33	0.24	6.37	0.24	Hornblende andesite dike of Markleeville Pk	Thadp
JHCP-44	Andesite	Hbl	38.7544	119.8969	na		10.70	0.10	10.77	0.10	Pyroxene andesite intrusion of Pickett Pk	Tpai
JHCP-14	Andesite	Hbl	38.7184	119.9853	na		13.51	0.16	13.61	0.16	Red Lake Pk hb andesite block-and-ash-flow tuff	Thaba2
JHCP-7	Andesite	Plag	38.6433	119.9037	na		15.4	0.6	15.5	0.6	Jeff Davis Pk pyx-hb andesite and dacite block-and-ash-flow tuff	Tphaba
(D) Northern Sierra: Lovejoy basalt and overlying strata at Red Clover Creek (Garrison <i>et al.</i> 2008)												
02BrRCC10a	Andesite	Plag	39.98858	120.5426	9.96	0.24	10.11	0.24	10.18	0.24	Hornblende andesite block-and-ash-flow tuff	Mhab
02BrRCC6	Andesite	WR	39.9822	120.5480	14.00	0.50	14.21	0.50	14.31	0.50	Plagioclase andesite breccia	Mpb
03LJSR13	Basalt	Plag	40.15567	120.48922	15.12	4.64	15.35	4.64	15.45	4.64	Proximal Lovejoy basalt (Stony Ridge) uppermost flow	
02LJRCC8-B	Basalt	Plag	39.98818	120.56505	15.30	2.58	15.53	2.58	15.63	2.58	Proximal Lovejoy basalt (Red Clover Creek) uppermost flow	Mlb
02LJRCC8-A	Basalt	Plag	39.98818	120.56505	15.60	1.00	15.84	1.00	15.94	1.00	Proximal Lovejoy basalt (Red Clover Creek) uppermost flow	Mlb

Table 1 – continued

Sample no.	Geochem	Mineral	Lat (°N)	Long (°W)	Interpreted age (Ma) <sup>a</sup>		Nominal age (Ma) <sup>b</sup>		Preferred age (Ma) <sup>c</sup>		Unit name	Map unit
					Age	±2s	Age	±2s	Age	±2s		
03LJSTM3	Basalt	WR	39.55137	121.57967	15.63	0.30	15.87	0.30	15.97	0.30	Distal coarse-grained Lovejoy basalt flow at South Table Mtn	
03LJSTM4	Basalt	WR	39.5498	121.57642	16.00	0.50	16.24	0.50	16.35	0.50	Distal coarse-grained uppermost flow South Table Mtn	
(E) Northern Sierra: Dixie Mountain Center (Roulet 2006)												
Dixie 90	Andesite	Plag	39.8559	120.33225	10.4	0.2	10.58	0.2	10.65	0.2	Hbl pyroxene andesite sill	Tuhpa
Dixie 2	Andesite	Plag	39.54081	120.17758	10.50	0.20	10.66	0.20	10.73	0.20	Hbl biotite andesite intrusions	Thbai
Dixie 245	Andesite	Plag	39.9372	120.3357	10.50	0.30	10.66	0.30	10.73	0.30	Block-and-ash-flow tuff	Tbaf2
Dixie 47b	Andesite	Plag	39.54721	120.17793	10.85	0.20	11.02	0.20	11.09	0.20	Block-and-ash-flow tuff	Tbaf1

<sup>a</sup>Interpreted age is calculated using 27.60 Ma for the Fish Canyon sanidine (FCs) standard as reported by Gans in Busby *et al.* (2008a,b), Garrison *et al.* (2008), and Roulet (2006).

<sup>b</sup>Nominal age is calculated using 28.02 Ma for the FCs standard (Renne *et al.* 1998).

<sup>c</sup>Preferred age is calculated using 28.201 Ma for the FCs standard (Kuiper *et al.* 2008).

### ***Oligocene–early Miocene ignimbrites in palaeochannels inherited from Cretaceous–Palaeocene time (sequence 1)***

Eocene sedimentary rocks that constitute the basal fill of palaeochannels cut into Cretaceous granitic basement of the Sierra Nevada have yielded indefinite results concerning the palaeogeography of the range (Cecil *et al.* 2007). These are mainly preserved in the palaeochannels of the northern Sierra, and not present in the central high Sierran palaeocanyons described here.

Much more clear are the implications of the presence of ~22–30 Ma ignimbrites in the palaeochannels (Figure 7, cross-section 1). These ignimbrites erupted from calderas situated in central Nevada (Garside *et al.* 2005; Henry 2008; Figure 2). For these to have flowed from central Nevada to the Sacramento Valley of central California, surface elevations must have continuously decreased in that direction, and the region could not have yet been disrupted by normal faults.

In the central Sierra Nevada, unconformity 1 is an extremely rugged surface, especially where it is cut into the metamorphic rocks, which form fins, but also where it is cut into the granitic rock, as shown in Figure 6(a). In this paper, we refer to the ignimbrites as sequence 1, because they overlie unconformity 1 in the high central Sierra. These ignimbrites generally have small pumices and few, small lithic fragments, consistent with their distal nature (Figure 6(b)). Although it is obvious from their mineralogy that several different ignimbrite sheets filled the palaeocanyons, we have not attempted to divide them, because they were largely eroded away during the development of unconformity 2 (described below).

### ***Eruption of 16 Ma flood basalts through incipient Sierran frontal fault***

The oldest Cenozoic volcanic rock that vented through what is now the Sierra Nevada is a flood basalt erupted from a fissure along the Honey Lake fault zone, in the northern Sierra just west of Honey Lake (Figures 2 and 5). The Lovejoy basalt is the largest known eruptive unit in California, and has geochemical affinities with coeval flood basalts of the Columbia River Group (Figure 1; Garrison *et al.* 2008).

The fissure vent for the Lovejoy basalt lies along one of the most important fault zones of the Walker Lane belt, the Honey Lake fault zone (Figure 5; also see Figure 7, cross-section 2, of Garrison *et al.* 2008). Unlike other Miocene flood basalts of the western USA, it was not erupted in a back-arc position, but rather at the front of the arc (see 15–20 Ma position of the arc front in Figure 2). The fissure that vented basalt magmas lies along the Honey Lake fault zone, suggesting that at least incipient mild extension, and perhaps some normal fault-related footwall uplift, occurred in the northern Sierra at about 16 Ma.

### ***Westward sweep of the Ancestral Cascades arc front into the Sierra Nevada at 16 Ma (sequence 2)***

In the central Sierra, ignimbrites that gradually accumulated over a long period (from ~30 to ~22 Ma, Figure 7, cross-section 1) were deeply dissected along unconformity 2 prior to the first pulse of arc volcanism, dated at 16–13 Ma (Figure 4). However, the ignimbrites were not dissected in the northern Sierra (see Figure 5 of Garside *et al.* 2005; Busby's unpublished mapping). This difference indicates that climatic change was not the primary control on the unconformity, since that would presumably affect both areas. For reasons given in this section, we infer that the control was thermo-tectonic (Figure 7, cross-section 3).

The Oligocene ignimbrites were virtually reamed out of the central Sierran palaeocanyons during the development of unconformity 2, leaving bits of their stratigraphy stranded on the palaeoedges, palaeowalls, and parts of the irregular palaeocanyon floors. Unconformity 2 is locally overlain by granitic boulder conglomerate (Figure 6(c)), suggesting at least local incision into bedrock at this time.

As noted above, recent stable isotope work has shown that the southwestward sweep of the arc through Idaho and Nevada was accompanied by synchronous extension and increase in surface elevation, interpreted to record thermal effects as the Farallon slab fell back (Horton and Chamberlain 2006; Kent-Corson *et al.* 2006; Mulch *et al.* 2007). By analogy, we suggest that unconformity 2 records the same process. We therefore assign an age of  $\sim 16$  Ma to this inferred uplift event, since that is the age of the westward sweep of the arc into the Sierra Nevada (Figure 7, cross-section 3). More local evidence for the timing of onset of extension (but without evidence for or against synchronous increase in surface elevation) comes from adjacent parts of Nevada. Extension in the Wassuk Range and the Singatse Range (Figure 5) is estimated to have occurred between about 15 and 14 Ma, and between about 15 and 12 Ma, respectively (Proffett 1977; Dilles and Gans 1995; Stockli *et al.* 2002; Surpless *et al.* 2002). This is similar to the age we infer for the development of unconformity 2 in the central Sierra.

The  $\sim 16$  Ma uplift event was followed by a period of tectonic quiescence in the central Sierra, when  $\sim 16$ –13 Ma volcanic rocks (Figure 4) and  $\sim 13$ –11 Ma fluvial and debris flow deposits of sequence 2 aggraded within palaeochannels, and no unconformities formed (Figure 7, cross-section 3) (Busby *et al.* 2008a,b; Hagan *et al.* 2009). Nonetheless, steep slopes persisted in the central Sierran palaeocanyons during the accumulation of sequence 2, as shown by the presence of avalanche megablocks (Figure 6(d)). Age controls on the first pulse of magmatism in the Sierra are the poorest of the three pulses (Figure 4) because the oldest volcanic rocks are the most altered, making it harder to find fresh samples suitable for dating (note the larger error on these ages).

Andesitic intrusive, volcanic, and volcanoclastic rocks of sequence 2 are not distinguishable from those of sequences 3 and 4 on the basis of any field, petrographic, or geochemical characteristics, with the notable exception of the distinctive high-K rocks of the Stanislaus Group around the Sonora Pass (described in sequence 3, below). Like the rest of the Miocene Ancestral Cascades arc rocks in the Sierra Nevada, sequence 2 includes shallow-level intrusions, block-and-ash-flow tuffs, volcanic debris flow deposits, and fluvial deposits, nearly all of the andesitic composition; lava flows are rare (Busby *et al.* 2008a,b). Petrified wood occurs in the debris flow deposits (Figure 6(e)) and charred wood occurs in the block-and-ash-flow tuffs. The block-and-ash-flow-tuffs are monomict (Figure 6(f)), and lack any pumice, indicating an origin by lava dome collapse. These are interstratified with and pass down-palaeocanyon into debris flow deposits, which in turn are interstratified with and pass down-palaeocanyon into fluvial deposits (Figure 6(g–i)). Well-stratified, well-sorted fluvial deposits with rounded clasts occur at all stratigraphic levels in sequence 2, including the base of the sequence (e.g. see volcanic fluvial conglomerate and sandstone unit Tvf1 of Hagan *et al.* 2009). This indicates that at least some of the sediment was derived from points east of the present-day Sierra Nevada, so our proposed  $\sim 16$  Ma thermal uplift/extensional event must not have disrupted drainages. One important difference between sequences 2, 3, and 4 is that sequences 2 and 3 have a much higher proportion of well-rounded, well-sorted fluvial deposits in what is now the crestral region of the Sierra; as discussed below, we infer that this records late Miocene beheading of the palaeocanyons from sources to the east in Nevada, due to range-front faulting.

Much less is known about rocks of sequence-2 age in the northern Sierra, due to a general lack of detailed maps and dates there, but Garrison *et al.* (2008) presented a single date of 14 Ma (Table 1) on an andesite flow breccia that lies upsection from the Lovejoy basalt at the Red Clover Creek (Figure 5).

### ***Dextral transtension and high-K volcanism: birth of the Sierra Nevada microplate at 11 Ma (sequence 3)***

Andesite volcanic and volcanoclastic rocks that steadily aggraded in the palaeochannels from ~16 to ~11 Ma were deeply incised along unconformity 3 before the onset of volcanic pulse 2 (Figure 7, cross-section 4), which spans ~10.7–9 Ma (Figure 4). Sequence 3 includes high-K lava flows and ignimbrites in the Sonora Pass to Ebbetts Pass region, and andesitic volcanic and volcanoclastic rocks in the Ebbetts Pass to Carson Pass region (Busby *et al.* 2008a,b; Hagan *et al.* 2009; and our unpublished mapping). Numerous workers have inferred that the high-K rocks erupted from the Little Walker Caldera, also referred to as the Little Walker Center (Slemmons 1966; Noble *et al.* 1974, 1976; Priest 1979; King *et al.* 2007; Putirka and Busby 2007; Busby *et al.* 2008b; Koerner *et al.* 2009; Pluhar *et al.* 2009).

We have direct evidence for the onset of dextral transtensional range-front faulting during the development of unconformity 3, immediately prior to the beginning of eruption of the high-K rocks. Busby *et al.* (2008b) mapped a series of east-dipping, down-to-the-east normal faults that step right round the Little Walker Center, including (from west to east) the St Mary's Pass fault, the Lost Cannon fault, the Grouse Meadow fault, and the Sonora Junction fault (Figure 5). A 500 m-thick avalanche deposit with blocks up to 1.6 km long was shed from the footwall of the St Mary's Pass fault onto its hanging wall within 140 kyr of the beginning of the high-K eruptions, as shown by ages on transported material in the avalanche blocks and on the basal unit of the high-K rocks (Table Mountain Latite lava flows; Busby *et al.* 2008b). Chaotically tilted strata in the landside blocks beneath the Table Mountain Latite are obvious from Highway 108, including views from the Sonora Pass northwards towards Sonora Peak (Figure 6(g)) and views east of the pass towards the south at Sardine Falls (Figure 6(j)). Along the next fault to the east, the Lost Cannon fault (Figure 5), sequence 1 and 2 strata are rotated much more steeply by the fault than the overlying Table Mountain Latite of sequence 3, and the sequence 2 andesitic volcanoclastic rocks contain avalanche blocks of sequence 1 ignimbrites, indicating that this fault also began to slip prior to the eruption of the high-K rocks (Busby *et al.* 2008b). Additional slip on that fault during the eruption of the Table Mountain Latite may be indicated by dramatic thickening of the lavas and interstratified fluvial sandstones towards the fault (Busby *et al.* 2008b). All of these faults were re-activated after emplacement of sequence 3 volcanic rocks, and some show evidence of Quaternary to Recent displacement; it was only through detailed mapping of the Miocene palaeocanyon fill that the 11 Ma initiation of this fault zone could be recognized. We thus infer that the Little Walker Caldera (Figure 5) was formed along a releasing stepover of this fault zone (Putirka and Busby 2007; Busby *et al.* 2008b).

Sequence 3 strata in the Sonora Pass area are dominated by the eruptive products of the Little Walker Center/Caldera. In its earliest activity, it was likely the source for the second largest known lava flow unit in California (after the Lovejoy basalt), the 10.4 Ma Table Mountain Latite (Table 1). The Table Mountain Latite consists of voluminous trachyandesite to trachybasaltic andesite lavas (Putirka and Busby 2007) that flowed westward through palaeochannels in the central Sierra Nevada to the Central Valley

(Ransome 1898; Slemmons 1953, 1966; Noble *et al.* 1974; Priest 1979; King *et al.* 2007; Gorny *et al.* 2009; Koerner *et al.* 2009; Pluhar *et al.* 2009). Flow within palaeoriver channels is indicated by the presence of blocky jointing on the tops of some flows (Figure 6(k)), suggesting quenching by water, and stretching of vesicles parallel to the trend of the palaeocanyon system (Figure 5(l)). At the present-day Sierran crest, the Table Mountain Latite consists of 23 lava flows and is over 400 m thick (Busby *et al.* 2008b). In its distal facies, 130 km to the west near Knight's Ferry, it is up to 45 m thick, and consists of one very thick flow and three much thinner flows with weathered tops, which palaeomagnetic data show all erupted in less than a few centuries (Gorny *et al.* 2009). The proximal facies of the Table Mountain Latite section locally has minor olivine basalt lava flows, which are useful for petrogenetic studies (Putirka and Busby 2007; Koerner *et al.* 2009; work in progress). The 10.4 Ma Table Mountain Latite is overlain by the 9.54–9.34 Ma Eureka Valley Tuff (Table 1), which consists of three trachydacite ignimbrite members (King *et al.* 2007; Koerner *et al.* 2009), also erupted from the Little Walker Caldera (Priest 1979; King *et al.* 2007). The lower two members of the Eureka Valley Tuff make a very distinctive black ledge across the landscape (Figure 6(m)), and also have distinctive black glassy fiamme on outcrop (Figure 6(n)). High-K lavas previously recognized between the lower two members of the Eureka Valley Tuff at the caldera (Priest 1979; Brem 1977) are also present in the Sierran palaeocanyon at Sonora Pass (Koerner *et al.* 2009). This unit, which we refer to as the Lava Flow Member of the Eureka Valley Tuff, includes both normal- and reversed-polarity lava flows (Pluhar *et al.* 2009), and ranges from trachyandesite to trachydacite in composition (Koerner *et al.* 2009). The Dardanelles Formation, which also consists of high-K lavas flows (trachyandesites or shoshonites), has long been inferred to lie above the Eureka Valley Tuff (Slemmons 1966; Noble *et al.* 1974, 1976), although no maps or measured sections were previously published to demonstrate that it lies above all three members of the Eureka Valley Tuff; previous workers have therefore confused it with the Lava Flow Member of the Eureka Valley Tuff or the Table Mountain Latite at some localities (Koerner *et al.* 2009). New mapping west of Sonora Pass demonstrates that trachyandesite lava flows do in fact overlie the upper member of the Eureka Valley Tuff (Koerner *et al.* 2009). The Dardanelles Formation is not yet dated, but its normal magnetic polarity suggests that it was erupted between 9.44 and 9.35 Ma, or else it is younger than 9 Ma (Pluhar *et al.* 2009). Together, all of these high-K volcanic rocks make up the Stanislaus Group, which we infer records low-degree partial melting of the mantle lithosphere along a pull-apart structure. We infer that the eruptive products of the Little Walker Caldera formed in a pull-apart basin bounded by releasing stepover faults that penetrated a lithospheric plate with a thick crustal section. These transtensional stresses resulted in the eruption of low-degree (high-K) partial melts (Putirka and Busby 2007) (Figure 7, cross-section 4), signalling the birth of the Sierra Nevada microplate (Figure 1). This ~10.5 Ma faulting clearly did not succeed in completely disrupting the palaeocanyon system, because the 10.4–9 Ma eruptive products were funnelled along it.

Unlike the Sonora Pass to Ebbetts Pass area, we cannot demonstrate a direct link between the faulting and development of unconformity 3 in the Carson Pass area (Hagan *et al.* 2009). However, just to the east in the Gardnerville Basin (Figure 5), gravity studies show evidence of older (pre-7 Ma) normal faults buried beneath the 7 Ma–Recent basin fill associated with the Genoa fault (Cashman *et al.* 2009). Perhaps these faults also record the birth of the Sierra Nevada microplate. There is no evidence for high-K volcanism in sequence 3 strata between Ebbetts Pass and Carson Pass. Instead, these strata consist largely of andesitic volcaniclastic debris and fluvial deposits reworked down-

palaeocanyon from sources to the east, indicating that the palaeocanyon system was not yet completely disrupted by faults. In addition, sequence 3 strata at Carson Pass contain proximal volcanic rocks, including block-and-ash-flow tuffs and peperitic intrusions (Busby *et al.* 2008a; Hagan *et al.* 2009).

We tentatively suggest that the 11–10 Ma initiation of the Sierra Nevada microplate is recorded in the Cenozoic strata of the northern Sierra (as well as the central Sierra). The Miocene rocks there have not been mapped in great detail, although a series of 1:62,500 and 1:100,000 maps are available from the California Geological Survey (Grose *et al.* 1990; Grose 2000a,b,c,d; Grose and Mergner 2000) and are very useful for selecting the key areas suitable for more detailed work. On the basis of more detailed (1:24,000 scale) mapping, we have preliminary evidence that the northern Sierra began to be broken into the structural blocks that define the northeastern boundary of the Sierra Nevada microplate at 11–10 Ma. Unpublished detailed mapping and dating of the Dixie Mountain centre area (Figure 5; Rouillet 2006) and unpublished reconnaissance mapping by Busby indicate that a section of andesitic volcanic debris flows, lesser block-and-ash-flow tuffs, and minor lava flows at least 500 m thick covers an area of at least 20 × 30 km. This section accumulated in less than 0.3 Myr (between 10.8 and 10.5 Ma, Table 1), which is a very high rate (1.6 mm/year). We tentatively propose that this section was accommodated by the subsidence of an intra-arc basin that formed between the Mohawk Valley and Honey Lake fault zones (Figure 5), although further mapping and dating are needed to better define this basin. The basin may thus record the beginning of dismemberment of what is now the northern Sierra along the northern boundary of the Sierra Nevada microplate. The Dixie Mountain centre, which intrudes this basin fill, is a 10.5 Ma laccolith that was emplaced mainly at the contact between the granitic basement and the volcanoclastic basin fill, and warped the fill upward off the basement. However, the laccolith also intruded up through the basin fill as a series of sills, ‘Christmas tree’ style, and it locally broke through the cover to vent block-and-ash flows into the basin (Rouillet 2006; C.J. Busby *et al.*, unpublished data). Intrusions of the Dixie Mountain centre extend about 13 km in a NNW–SSE direction and about 9 km in a WSW–NE direction, suggesting a structural control on its position and shape.

An ~10–11 Ma age for the birth of the Sierran microplate is supported by studies from many other parts of the Sierra Nevada and adjacent regions. On the north side of present-day Lake Tahoe (Figure 1), the Verdi-Boca Basin formed at ~12 Ma, along the down-to-the-east Donner Pass fault (Henry and Perkins 2001). This fault forms part of the Tahoe–Sierra frontal fault zone of Schweickert *et al.* (1999, 2000, 2004), which runs up the west side of Lake Tahoe. Across Lake Tahoe to the east in the Carson Range, Tertiary strata useful for determining direction and timing of tilting are rare, but Surpless *et al.* (2002) modelled thermochronological data to infer a 15°-westward tilting of the Carson Range, at about 10–3 Ma. In the southern Sierra Nevada, He apatite data from the footwall of the Mount Whitney escarpment indicate rapid tectonic denudation at ~10 Ma (Mahéo *et al.* 2004). The Indian Wells segment of the eastern escarpment of the southern Sierra Nevada shed sediment into the El Paso basin by ~8 Ma (Loomis and Burbank 1988). Finally, a massive sand sheet in the San Joaquin basin records a ~10 Ma phase of uplift and incision of southern Sierran granitic basement (Saleeby *et al.* 2009); by contrast, basement incision in the central to northern Sierra basement was delayed until Pliocene time. As discussed below, we infer that it was delayed there because base level in the adjacent Great Valley was raised dramatically by the production of a volcanoclastic fluvial wedge. Saleeby *et al.* (2009) infer that the ~10 Ma event resulted in the westward tilting and uplift that was to a first order uniform along the length of the microplate, producing an

elevation increase of  $\sim 1000$  m along the eastern Sierra crest. We argue below that this fundamental, plate margin-scale event is what produced unconformity 3, rather than other possible controls, such as fluctuations in sediment supply or climate.

#### ***Renewed extension, rejuvenation, and beheading of palaeocanyons, and 7–6 Ma volcanism (sequence 4)***

Our age constraints on the timespan covered by unconformity 4 are as follows: It cuts the  $\sim 10.5$ –9 Ma volcanic rocks, and is overlain by volcanic rocks as old as 7 Ma (Busby *et al.* 2008a). However, in the Ebbetts Pass area, the 9 Ma rocks are overlain by a thick, undated section of andesitic fluvial and debris flow deposits (Keith *et al.* 1982), so we prefer the interpretation that the unconformity formed between 7 and 8 Ma. We infer that unconformity 4 records renewed range-front faulting (and possible footwall uplift) at about 7–8 Ma (Figure 7, cross-section 5).

Range-front faults clearly controlled the positions of volcanic centres during magmatic pulse 3. One of the bigger volcanic centres recognized in the Sierra, the Markleeville Center, developed within the Hope Valley graben at Carson Pass at this time (CP, Figure 2). This centre is about 8 km in diameter and consists of hornblende dacite and andesite intrusions and altered roof rocks (Hagan *et al.* 2009). Sequence 4 andesite lava flows also erupted along this fault zone, and andesites intruded fault breccias in the granitic basement (Hagan *et al.* 2009). The next fault to the east of the Hope Valley graben, which we name the Grover Hot Springs fault (J. Hagan and C.J. Busby, unpublished mapping), extends southwards to Ebbetts Pass (Armin *et al.* 1984) where it overlaps with the Noble Canyon fault of Armin *et al.* (1984) (Figure 5). Activity on the Grover Hot Springs and Noble Canyon fault overlapped in time as well as space (J. Hagan and C.J. Busby, unpublished mapping). Immediately south of the area of fault overlap, in the Ebbetts Pass palaeocanyon, lies a landslide deposit several hundred metres thick, composed of chaotic andesitic strata. We infer that this landslide deposit was shed from the area of fault overlap, due to tilting along the lateral ramp, because granitic basement rocks and sequence 1 Oligocene ignimbrites are exhumed and Miocene arc strata are missing on the ramp. This exhumed basement thus forms part of unconformity 4. The ramp then acted as a sediment transfer path for very large granitic boulders that were funnelled into sequence 4 strata of the Ebbetts Pass palaeocanyon (Figure 6(o)). Sequence 4 breccias at Ebbetts Pass are the coarsest of any sequence in the central Sierran palaeocanyons (Figure 6(p)). The Grover Hot Springs fault (and a shorter fault to the east of it, the Silver Mountain fault, Figure 5) controlled the siting of a 10 km-diameter volcano, which we call the Ebbetts Pass Center (J. Hagan and C.J. Busby, unpublished mapping). This volcano consists of radially dipping basaltic andesite lava flows, with a dacitic intrusive core that sits directly above the projected trace of the Grover Hot Springs fault (Figure 6(q); Hagan, Busby, Putirka and Renne, unpublished mapping, geochemistry and dating in progress). Although this volcano is not yet dated, map relations suggest that it forms a part of the 7–6 Ma magmatic pulse (sequence 4). The Nobel Canyon fault shows evidence of minor reactivation after the volcano formed, because it offsets the western margin of the volcano by about 100 m (J. Hagan and C.J. Busby, unpublished mapping).

Unconformity 4 is the deepest and steepest-sided Miocene unconformity in the central Sierra. In places, it downcuts into granitic basement and it formed local slopes of up to  $48^\circ$ , representing very steep palaeocanyon walls in the late late Miocene. Mass wasting deposits are common in sequence 4, and include slide and avalanche blocks hundreds of metres in size (I. Skilling and C. Busby, unpublished mapping). Some of the larger slide

blocks consist of lithified sequence 3 debris flow deposits complete with their 10–11 Ma andesitic intrusions, described *in situ* by Busby *et al.* (2008a) and Hagan *et al.* (2009). These steep-sided canyons, prone to mass failure, were more like gullies than channels, because they served less as fluvial conduits than as depocentres for locally sourced breccias, debris flow deposits, lava flows, and block-and-ash-flow tuffs. Sequence 4 lacks the andesitic fluvial sandstones and conglomerates that occur at all stratigraphic levels in the other Miocene sequences (2 and 3). We interpret this to mean that the palaeocanyons were beheaded by the range-front faults by this time.

### ***Post-Miocene faulting***

Some of the faults that we infer were active during the development of unconformities 2, 3, and 4 were clearly reactivated at some time after arc volcanism ceased at ~6 Ma due to passage of the triple junction (Figure 1), since they offset the youngest volcanic deposits. Some remain active today; for example, the Sonora Junction fault (Figure 5) has fresh scarps along it. Similarly, the Genoa fault (Figure 5), which has active seismicity, began to slip at 7 Ma (Cashman 2009). It is not known whether the range-front zone remained continuously active, or moved episodically between 6 Ma and present. However, the deposits of sequence 4 are cut by the modern canyons of the Sierra Nevada, so faulting and tilting have occurred since Miocene time.

### **Significance of unconformities**

We recognize three Miocene unconformities, each 300–600 m deep (vertical distance from top to bottom), in the central Sierra Nevada. These are too deep to be the result of eustatic base-level changes, so they must record changes in climate or sediment supply, or have fundamentally tectonic controls.

Existing climate data from the western USA do not suggest any dramatic changes that could easily explain the unconformities. Horton and Chamberlain (2006) instead suggest that gradual climate change occurred since the middle Miocene in the form of prolonged cooling and aridification, consistent with marine climate records that indicate an ~5°C drop in temperature. They also discounted the importance of any palaeolatitudinal changes on climate, because the western USA has been at about the same latitude throughout the Cenozoic (Horton and Chamberlain 2006). Furthermore, Mulch *et al.* (2008) have recently used hydrogen isotope data on hydrated glasses to infer that climate and precipitation patterns have not changed substantially over the last 12 Myr or more. Last, as argued above, it seems unlikely that climate change was the main control on the erosion of unconformity 2, because it is very strongly developed in the central Sierra, and is virtually absent in the northern Sierra; a change in climate would have presumably affected both the areas.

One possibility invoked for the origin of unconformities in other volcanic terranes is eruption-induced aggradation, in the form of catastrophic sedimentation triggered by explosive eruptions, followed by dissection to base level when the explosive volcanism ends (Smith and Lowe 1991). The palaeochannel fill of the central Sierra Nevada does not fit this model for two reasons: (1) The aggradation–reincision events predicted by an eruption-induced mechanism occur on a short time scale (that of the activity and dormancy of a volcano, which is typically much less than 10 kyr in arc volcanoes), and are dominated by explosive volcanic products. Although the Oligocene to early Miocene aggradational event was fed from explosive eruptions, aggradation was ongoing for at least 8 Myr before

dissection began in the central Sierra. (2) The palaeochannel fill for the younger two (Miocene) aggradation events lacks explosive volcanic products, and although some of its fill is catastrophic in nature (lava flows and debris flows), much of its fill is non-catastrophic in nature (fluvial conglomerate and sandstone), with sedimentary structures that suggest steady, prolonged aggradation. These aggradational events spanned  $\sim 5\text{--}2.5$  Myr.

It has been argued that the only unconformity that can be used to infer Cenozoic uplift of the Sierra Nevada is the post-5 Ma unconformity, because that is the only one that incises through Cenozoic strata into the basement rocks (Wakabayashi and Sawyer 2001). This interpretation makes the assumption that base level (the lowest point to which a stream can flow) has been the same for the Sierran rivers ever since Cretaceous or Palaeocene time. This is a reasonable assumption for periods of time when Sierran rivers had their mouths at the sea, as recorded in the marine Eocene Ione Formation of the westernmost Sierra Nevada foothills. However, the Oligocene and Miocene rivers of the northern and central Sierra north of latitude  $37^\circ$  debouched into a nonmarine basin in the California Central Valley (Repenning 1960; Bartow 1991). We infer that base level rose in the Central Valley in Oligocene-to-early-Miocene time, due to transport of voluminous volcanoclastic sediment through palaeochannels from volcanoes in western Nevada, before the  $\sim 16$  Ma uplift event occurred in the central Sierra Nevada. Furthermore, we suggest that the base level continued to rise as even more voluminous volcanoclastic sediment was supplied to the channels from the Ancestral Cascades arc volcanoes in the northern and central Sierra Nevada, during the time that the next two uplift events occurred (at  $\sim 11$  and  $\sim 8$  Ma). We suggest that the nonmarine volcanoclastic wedge backfilled the lower reaches of the palaeocanyons and spread across the foothills, raising base level by hundreds of metres. This model could be tested through apatite He dating on the granitic basement, to look for age patterns indicative of differential disturbance due to thermal blanketing by sediment burial (Shuster *et al.* 2006; Flowers *et al.* 2007), similar to that found in the southern Sierra by Mahéo *et al.* (2009).

If the unconformities simply record re-incision after a canyon has been filled, we see no reason why the unconformities should be of the same age in all of the palaeocanyons, since different materials were supplied to different palaeocanyons at different times, and downcutting through a lava flow should take a great deal longer than downcutting through unlithified sands or gravels. Similarly, if an incision occurred in response to a change in sediment flux, the timing of this should vary from palaeocanyon to palaeocanyon, because of the rapidly shifting nature of the volcanic activity in the headwaters of the palaeocanyons. Thus, we consider it most likely that the unconformities formed in response to the coeval episodes of Miocene faulting, which we have clear evidence for, and we infer that footwall uplift produced the unconformities. This is consistent with the surface process modelling results of Pelletier (2007), which identifies two major pulses of surface uplift for the Sierra Nevada: one in the Latest Cretaceous, and one in the Miocene ( $\sim 15\text{--}10$  Ma).

### **The shape of the Cretaceous high plateau and its influence on Cenozoic landscape evolution**

We have previously inferred that a north-to-south decrease in Ancestral Cascades arc volcanic rocks (Figure 1) and a concomitant increase in the potassium content of these magmas in the Sierra Nevada were controlled by a marked north-to-south increase in the thickness of the low-density crust, which is reflected in a southward increase in the present-day summit elevations (Putirka and Busby 2007). Consistent with this interpretation are our findings that: (1) palaeorelief, defined as a relief that pre-dates Cenozoic deposits, increases

southwards within the range (Bateman and Wahrhaftig 1966; Wakabayashi and Sawyer 2001; Busby *et al.* 2008a), (2) the palaeochannels in the northern Sierra are broader and more flat-floored than the palaeocanyons in the central Sierra, which locally show slopes up to 50° on the granitic basement (Busby *et al.* 2008a), (3) the unconformities produced by Miocene re-incision events in palaeochannels of the northern Sierra are less than 15 m deep (vertical distance of erosion), even though the deposits are of similar thickness to the ones in the central Sierra (Wakabayashi and Sawyer 2001), while in the central Sierra palaeocanyons the Miocene unconformities are ~ 400–600 m deep (Busby *et al.* 2008a,b; Hagan *et al.* 2009), and (4) fluvial deposits in the central Sierran palaeocanyons are much coarser than they are in the northern Sierran palaeochannels, indicating higher axial gradients; also, mass-wasting deposits, which are common in the central Sierran palaeocanyons, have not been reported from the northern Sierran palaeochannels.

North of the northern Sierra Nevada, voluminous Late Cretaceous batholith rocks curve eastwards into northwest Nevada (Figure 1) where the crust was extended only a minor amount (< 15–20%), and is relatively thin (Lerch *et al.* 2008). Like the northern Sierra, Miocene volcanic–volcaniclastic strata in northwest Nevada are widespread, in contrast to the central Sierra where volcanic strata are preserved in palaeochannels; this indicates low palaeorelief.

Taken together, the field and geochemical data suggest that the edge of the Cretaceous ‘Nevadaplano’ (DeCelles 2004) decreased in the elevation northwards between the central and northern Sierra, and that its edge curved northeastwards through northwest Nevada. Thus, the highest part of the ‘Nevadaplano’ corresponds in part to the region of large-magnitude (~ 100%) Cenozoic synvolcanic extension, although it was broader, reaching northwards as far as Reno (Figure 1; Gans *et al.* 1989; Axen *et al.* 1993; Dickinson 2006), with an areal extent that was possibly controlled by the Palaeozoic palaeoedge of the North American continent. Sediment eroded off the high plateau may have drained northwards as well as westwards, into the Hornbrook basin of southeastern Oregon as well as the Central Valley of California (Figure 1). The north-draining palaeochannels, if they exist, are covered by the Pliocene to Recent Cascades arc volcanic rocks, with the possible exception of the ‘Jura River’, described in Lindgren’s classic 1911 study as a northward-draining palaeochannel in the northern Sierra (Figure 2; Lindgren 1911). Lindgren contrasted the fine-grained deposits of this river, sand and lignite, with the coarser fill of the west-flowing palaeochannels. This is consistent with our view that the central Sierran features are more aptly termed ‘palaeocanyons’ for their ruggedness, deep unconformities, and coarse fill (Busby *et al.* 2008a), while the northern Sierran palaeochannels developed on gentler slopes.

## Conclusions

A great deal of effort has been invested in applying modern laboratory and geophysical techniques to understand the Sierra Nevada, yet some of our most unambiguous constraints on Sierran landscape evolution derive from field studies of Cenozoic strata. New geologic data constrain the timing and nature of magmatic and sedimentary events, faulting, and possible uplift, thus providing a new and important context for laboratory and geophysical studies.

Geologic work in the Sierra Nevada shows that neither end-member model is correct for the debate regarding the youth vs. antiquity of the range. Many features of the Cenozoic palaeocanyons and palaeochannels reflect shape of the Cretaceous orogen (unconformity 1), but they were also affected by Miocene tectonic and magmatic events, in addition to

Pliocene to Recent events, not discussed here. In the central Sierra Nevada, we infer that faulting and possible uplift immediately preceded three arc volcanic pulses (at about 16, 11, and 8 Ma). These Miocene uplift events did not produce unconformities that cut down below Cretaceous–Palaeocene unconformity, because base level was raised in the Central Valley by the construction of a very thick nonmarine volcanoclastic wedge.

The fill of the palaeocanyons (where they have been studied in detail, near the present-day Sierran crest) records the progressive dismemberment of the Nevadaplano and, ultimately, canyon beheading. Sequence 1 is composed entirely of material (Oligocene ignimbrite) sourced from the highest part of the Nevadaplano. This material gradually filled the palaeocanyons over about 10 Myr. Sequences 2 and 3 (early and middle late Miocene) contain a mixture of vent–proximal volcanic rocks and fluvial sediment derived from more distant sources, presumably in Nevada. Sequence 4 (late late Miocene) is floored by a rugged, deep unconformity, and lacks the fluvial sediment derived from more distal sources; it records rejuvenation of the palaeocanyons, presumably by crestal uplift along range-front faults, and their beheading.

Although detailed mapping and dating are still in progress, we tentatively offer the following model for the Miocene structural evolution of the central-to-northern Sierra Nevada range:

1. Regional normal faulting at about 16–15 Ma was synchronous with the development of unconformity 2, followed by the onset of arc volcanism. Although we have not yet identified normal faults of this age along the Sierra Nevada range front, the incipient Honey Lake fault zone controlled the emplacement of basalt fissures in the northern Sierra at this time, and normal faults of similar age have been dated in some of the ranges immediately to the east of the central Sierra. We would expect this extension to have covered a relatively broad area but perhaps be the weakest of the three Miocene faulting events, if it was caused by stretching over a region of thermal uplift.
2. Regional range-front faulting at 11 Ma occurred synchronously with the development of unconformity 3, followed immediately by high-K volcanism. This records the birth of the ‘future plate boundary’ along the east margin of the Sierra Nevada microplate. This plate boundary was born in the axis of the Ancestral Cascades arc along the central Sierran range-front faults, during large-volume, high-K eruptions at the Little Walker Caldera (Putirka and Busby 2007; Busby *et al.* 2008b). The 11 Ma event was a plate-margin-scale event.
3. Range-front faulting resumed at about 8–7 Ma, synchronous with the development of unconformity 4. These faults controlled the siting of volcanoes, and some faults were re-activated, offsetting the volcanoes.

By analogy with the ~11 Ma event, we speculate that high-K volcanic rocks in the southern part of the range mark the inception of yet a fourth pulse of range-front faulting, at 3–3.5 Ma.

Our data from the central Sierra show that each of these range-front faulting episodes was synchronous with the development of an unconformity in the palaeocanyons, and was closely followed by emplacement of Ancestral Cascades arc intrusions and volcanic rocks. We therefore consider these to be related events and infer a primarily tectonic control on the development of the unconformities.

Whether or not the interpretation of a fundamentally tectonic control on the unconformities is accepted by future workers, we have clearly demonstrated that the Sierra Nevada cannot be regarded as a passive shoulder to the Nevadaplano in Miocene time. By

mapping and dating Cenozoic strata in detail, we have shown that what is now the Sierra Nevada was partly shaped by Miocene structural and magmatic events. This must be taken into consideration in any models put forward for the origin of the range.

### Acknowledgements

This research was supported by the National Science Foundation grant EAR-01252 (to Busby, Gans, and Skilling), EAR-0711276 (to Putirka and Busby), and EAR-0711181 (to Busby). Many of the field relations described in this paper drew upon thesis geologic mapping supervised by Busby, including Steve DeOreo (MS), Noah Garrison (MS), Fabrice Rouillet (MS), Carolyn Gorny (BS), Jeanette Hagan (PhD expected), and Alice Koerner (PhD expected). We thank the USGS EDMAP programme for supporting some of this work, through award numbers 03HQAG0030, 05GQAG0010, and 06HQAG0061 (to Busby). We thank the following people for valuable field discussions in the Sierra Nevada (while not holding them responsible for our interpretations): George Bergantz, Woody Brooks, Brian Cousens, Garniss Curtis, Jim Faulds, Larry Garside, Trobe Grose, Brian Hausback, Chris Henry, Angela Jayko, Nathan King, Christopher Pluhar, Dylan Rood, Jason Saleeby, Zorka Saleeby, George Saucedo, Ian Skilling, Burt Slemmons, Greg Stock, Jeff Tolhurst, David Wagner, and John Wakabayashi. Office discussions with Pat Cashman, Richard Fisher, Cliff Hopson, Paul Renne, and Rich Schweickert have also been valuable. Comments from two anonymous reviewers on an earlier version of this manuscript, and reviews from Jason Saleeby and Jeanette Hagan are kindly acknowledged. All of the 2006–2008 age data summarized in Table 1 were recalculated by Paul Renne (Berkeley Geochronology Center), and the 2009 data (Hagan *et al.* 2009) are his new dates; we are grateful to him for his careful attention to this matter. We thank Gerardo Torrez for his aid in the geochemical analysis, and Jeanette Hagan for drafting Figure 5.

### References

- Argus, D.F., and Gordon, R.G., 1991, Current Sierra Nevada-North America motion from very long baseline interferometry: Implications for the kinematics of the Western United States: *Geology*, v. 19, p. 1085–1088.
- Armin, R.A., John, D.A., Moore, W.J., and Dohrenwend, J.C., 1984, Geologic map of the Markleeville 15 Minute Quadrangle, Alpine County, California: Department of the Interior – United States Geological Survey.
- Axen, G.J., Taylor, W.J., and Bartley, J.M., 1993, Space-time patterns of the onset of extension and magmatism, southern Great Basin, Nevada, Utah and California: *Geological Society of America Bulletin*, v. 105, p. 56–76, doi:10.1130/0016-7606(1993)105<0056:STPATC>2.3.CO;2, 1993.
- Bartow, J.A., 1991, The Cenozoic evolution of the San Joaquin Valley, California: U.S. Geological Survey Professional Paper 1501.
- Bateman, P.C., and Wahrhaftig, C., 1966, Geology of the Sierra Nevada, in Bailey, E.H., ed., *Geology of northern California*: California Division of Mines Bulletin, v. 190, p. 107–172.
- Bennett, R.A., Davis, J.L., and Wernicke, B.P., 1999, Present-day pattern of Cordilleran deformation in the western United States: *Geology*, v. 27, p. 371–374.
- Brem, G.F., 1977, Petrogenesis of late Tertiary potassic volcanic rocks in the Sierra Nevada and western Great Basin [PhD dissertation]: University of California, Riverside.
- Busby, C.J., and Bassett, K., 2007, Volcanic facies architecture of an intra-arc strike-slip basin, Santa Rita Mountains, Arizona: *Bulletin of Volcanology*, v. 70, no. 1, p. 85–103.
- Busby, C., DeOreo, S., Skilling, I., Gans, P., and Hagan, J., 2008a, Carson Pass-Kirkwood paleocanyon system: Implications for the Tertiary evolution of the Sierra Nevada, California: *Geological Society of America Bulletin*, v. 120, nos. 3/4, p. 274–299.
- Busby, C.J., Hagan, J., Putirka, K., Pluhar, C., Gans, P., Rood, D., DeOreo, S., Skilling, I., and Wagner, D., 2008b, The ancestral Cascades arc: Implications for the development of the Sierran microplate and tectonic significance of high K<sub>2</sub>O volcanism, in Wright, J., and Shervais, J., eds., *Ophiolites, Arcs and Batholiths*: Geological Society of America Special Paper 438, p. 331–378.
- Cashman, P.H., Trexler, J.H., Muntean, T.W., Faulds, J.E., Louie, J.N., and Oppliger, G., 2009, Neogene tectonic evolution of the Sierra Nevada – Basin and Range transition zone at the latitude of Carson City, Nevada, in Oldow, J., and Cashman, P., eds., *Late Cenozoic structure*

- and evolution of the Great Basin-Sierra Nevada transition: Geological Society of America Special Paper 447, p. 171–188.
- Cecil, M.R., Ducea, M.N., Reiders, P.W., and Chase, C.G., 2007, Cenozoic exhumation of the northern Sierra Nevada, California, from (U-Th)/He thermochronology: Geological Society of America Bulletin, v. 118, p. 1481–1488.
- Christensen, M.N., 1966, Late Cenozoic crustal movements in the Sierra Nevada of California: Geological Society of America Bulletin, v. 77, p. 163–181.
- Clark, M.K., and Farley, K.A., 2007, Sierra Nevada river incision from apatite  $^4\text{He}/^3\text{He}$  thermochronometry: Eos, v. 88, F2186.
- Clark, M.K., Mahéo, G., Saleeby, J., and Farley, K.A., 2005, The non-equilibrium landscape of the southern Sierra Nevada, California: GSA Today, v. 15, p. 4–10.
- Cousens, B., Prytulak, J., Henry, C., Alcazar, A., and Brownrigg, T., 2008, Geology, geochronology, and geochemistry of the Mio-Pliocene Ancestral Cascades arc, northern Sierra Nevada, California and Nevada: The roles of the upper mantle subducting slab, and the Sierra Nevada lithosphere: Geosphere, v. 4, p. 829–853.
- DeCelles, P.G., 2004, Late Jurassic to Eocene evolution of the Cordilleran thrust belt and foreland basin system, western USA: American Journal of Science, v. 304, p. 105–168.
- Dickinson, W.R., 1997, Tectonic implications of Cenozoic volcanism in coastal California: Geological Society of America Bulletin, v. 109, p. 936–954.
- Dickinson, W.R., 2006, Geotectonic evolution of the Great Basin: Geosphere, v. 2, no. 7, p. 353–368, doi: 10.1130/GES00054.1.
- Dilles, J.H., and Gans, P.B., 1995, The chronology of Cenozoic volcanism and deformation in the Yerington area, western Basin and Range and Walker Lane: Geological Society of America Bulletin, v. 107, p. 474–486.
- Dixon, T.H., Miller, M., Farina, F., Wang, H., and Johnson, D., 2000, Present-day motion of the Sierra Nevada block and some tectonic implications for the Basin and Range province, North American Cordillera: Tectonics, v. 19, p. 1–24.
- Ducea, M.N., and Saleeby, J.B., 1996, Buoyancy sources for a large, unrooted mountain range, the Sierra Nevada, California: Evidence from xenolith thermobarometry: Journal of Geophysical Research, v. 101, p. 8229–8244.
- Ducea, M.N., and Saleeby, J.B., 1998, A case for delamination of the deep batholithic crust beneath the Sierra Nevada: International Geology Review, v. 40, p. 78–93.
- Flowers, R.M., Shuster, D.L., Wernicke, B.P., and Farley, K.A., 2007, Radiation damage control on apatite (U-Th)/He dates from the Grand Canyon region: Colorado Plateau, Geology, v. 35, no. 5, p. 447–450.
- Gans, P.B., Mahood, G.A., and Schermer, E., 1989, Synextensional magmatism in the Basin and Range province: A case study from the eastern Great Basin: Geological Society of America Special Paper, v. 233, p. 1–53.
- Garrison, N., Busby, C.J., Gans, P.B., Putirka, K., and Wagner, D.L., 2008, A mantle plume beneath California? The mid-Miocene Lovejoy flood basalt, northern California, in Wright, J., and Shervais, J., eds., Ophiolites, Arcs and Batholiths: A tribute to Cliff Hopson: Geological Society of America Special Paper 438, p. 551–572.
- Garside, L.J., Henry, C.D., Faulds, J.E., and Hinz, N.H., 2005, The upper reaches of the Sierra Nevada auriferous gold channels, in Rhoden, H.N., ed., Window to the World, Geological Society of Nevada Symposium Proceedings, May 14–18, 2005.
- Gorny, C., Busby, C., Pluhar, C.J., Hagan, J., and Putirka, K., 2009, An in-depth look at distal Sierra Nevada paleochannel fill: drill cores through the Table Mountain Latite near Knight's Ferry: International Geology Review, v. 51, DOI: 10.1080/00206810902944960.
- Grose, T.L.T., 2000a, Geologic map of the Portola 15' Quadrangle, Plumas County, California: California Department of Conservation, Division of Mines and Geology Open File Report, scale 1:62,500.
- Grose, T.L.T., 2000b, With contributions from Durrell, C., and D'Allura, J.A., Geologic map of the Blairsden 15' Quadrangle, Plumas County, California: California Department of Conservation, Division of Mines and Geology Open File Report, scale 1:62,500.
- Grose, T.L.T., 2000c, Geologic map of the Loyalton 15' Quadrangle, Plumas and Sierra Counties, California: California Department of Conservation, Division of Mines and Geology Open File Report, scale 1:62,500.

- Grose, T.L.T., 2000d, Geologic map of the Sierraville 15' Quadrangle, Sierra and Plumas Counties, California: California Department of Conservation, Division of Mines and Geology Open File Report, scale 1:62,500.
- Grose, T.L.T., and Mergner, M., 2000, Geologic map of the Chilcoot 15' Quadrangle Lassen and Plumas Counties, California: California Department of Conservation, Division of Mines and Geology Open File Report, scale 1:62,500.
- Grose, T.L.T., Wagner, D.L., Saucedo, G.J., and Medrano, M.D., 1989, Geologic map of the Doyle 15-minute quadrangle, Lassen and Plumas Counties, California: California Department of Conservation, Division of Mines and Geology Open-File Report 89-31, scale 1:62,500.
- Grose, T.L.T., Saucedo, G.J., and Wagner, D.L., 1990, Geologic map of the Susanville Quadrangle, Lassen County, California: California Department of Conservation, Division of Mines and Geology Open-File Report 91-01, scale 1:100,000.
- Hagan, J.C., Busby, C.J., Putirka, K., and Renne, P.R., 2009, Cenozoic palaeocanyon evolution, Ancestral Cascades arc volcanism, and structure of the Hope Valley-Carson Pass region, Sierra Nevada, California: *International Geology Review*, v. 51, DOI: 10.1080/00206810903028102.
- Hamilton, W., and Myers, W.B., 1966, Cenozoic tectonics of the western United States: *Reviews of Geophysics*, v. 4, p. 509–549.
- Henry, C.D., 2008, Ash-flow tuffs and paleovalleys in northeastern Nevada: Implications for Eocene paleogeography and extension in the Sevier hinterland, northern Great Basin: *Geosphere*, v. 4, p. 1–35.
- Henry, C.D., and Perkins, M.E., 2001, Sierra Nevada – Basin and Range transition near Reno, Nevada: Two-stage development at 12 and 3 Ma: *Geology*, v. 29, p. 719–722.
- Horton, T.W., and Chamberlain, C.P., 2006, Stable isotopic evidence for Neogene surface dropdown in the central Basin and Range Province: *GSA Bulletin*, v. 118, p. 475–490.
- Horton, T.W., Sjöstrom, D.J., Abruzzese, M.J., Poage, M.A., Waldbauer, J.R., Hren, M., Wooden, J., and Chamberlain, C.P., 2004, Spatial and temporal variation of Cenozoic surface elevation in the Great Basin and Sierra Nevada: *American Journal of Science*, v. 304, p. 862–888.
- House, M.A., Wernicke, B.P., and Farley, K.A., 1998, Dating topography of the Sierra Nevada, California, using apatite (U-Th)/He ages: *Nature*, v. 396, p. 66–69.
- House, M.A., Wernicke, B.P., and Farley, K.A., 2001, Paleo-geomorphology of the Sierra Nevada, California, from (U-Th)/He ages in apatite: *American Journal of Science*, v. 301, p. 77–102.
- Huber, N.K., 1981, Amount and timing of late Cenozoic uplift and tilt of the central Sierra Nevada, California—Evidence from the upper San Joaquin river basin: *US Geological Survey Professional Paper 1197*, p. 1–28.
- Jones, C.H., Farmer, G.L., and Unruh, J.R., 2004, Tectonics of Pliocene removal of lithosphere of the Sierra Nevada, California: *Geological Society of America Bulletin*, v. 116, p. 1408–1422.
- Keith, W.J., Dohrenwend, J.C., Guisso, J.R., and John, D.A., 1982, Geologic map of the Carson-Iceberg and Leavitt Lake Roadless Areas, central Sierra Nevada, California: *US Geological Survey Report MF-1416-A*, scale 1:62,500.
- Kent-Corson, M.L., Sherman, L.S., Mulch, A., and Chamberlain, C.P., 2006, Cenozoic topographic and climatic response to changing tectonic boundary conditions in Western North America: *Earth and Planetary Science Letters*, v. 252, p. 453–466.
- King, N.M., Hillhouse, J.W., Gromme, S., Hausback, B.P., and Pluhar, C.J., 2007, Stratigraphy, paleomagnetism, geochemistry, and anisotropy of magnetic susceptibility of the Miocene Stanislaus Group, central Sierra Nevada and Sweetwater Mountains, California and Nevada: *Geosphere*, v. 3, no. 6, p. 646–666.
- Koenig, J.B., 1963, Geologic map of California: Walker Lake sheet: *California Division of Mines and Geology*, scale 1:250,000.
- Koerner, A., Busby, C., Putirka, K., and Pluhar, C.J., 2009, New evidence for alternating effusive and explosive eruptions from the type section of the Stanislaus Group in the 'Cataract' palaeocanyon, central Sierra Nevada: *International Geology Review*, v. 51, doi:10.1080/00206810903028185.
- Kuiper, K.F., Deino, A.L., Krijgsman, W., Renne, P.R., and Wijbrans, J.R., 2008, Synchronizing the rock clocks of Earth history: *Science*, v. 320, p. 500–504.
- Lerch, D.W., Miller, E., McWilliams, M., and Colgan, J., 2008, Tectonic and magmatic evolution of the northwestern Basin and Range and its transition to unextended volcanic plateaus: Black Rock Range, Nevada: *Geological Society of America Bulletin*, v. 120, p. 300–311.

- Lindgren, W., 1911, The Tertiary Gravels of the Sierra Nevada of California: Washington, DC: United States Geological Survey, p. 1–222.
- Loomis, D.P., and Burbank, D.W., 1988, The stratigraphic evolution of the El Paso Basin, Southern California; implications for the Miocene development of the Garlock Fault and uplift of the Sierra Nevada: Geological Society of America Bulletin, v. 100, p. 12–28.
- Mahéo, G., Farley, K.A., Clark, M.K., and Shuster, D., 2004, Cooling and Exhumation of the Sierra Nevada Batholith in the Mount Whitney Area (California) Based on (U-Th)/He Thermochronometry: American Geophysical Union, Abstract T41D-1252, San Francisco.
- Mahéo, G., Saleeby, J., Saleeby, Z., and Farley, K.A., 2009, Tectonic control on Southern Sierra Topography, California: Tectonics (in press).
- Mulch, A., Graham, S.A., and Chamberlain, C.P., 2006, Hydrogen isotopes in Eocene river gravels and paleoelevation of the Sierra Nevada: Science, v. 313, no. 87, p. 87–89.
- Mulch, A., Teyssier, C., Cosca, M.A., and Chamberlain, C.P., 2007, Stable isotope paleoaltimetry of Eocene core complexes in the North American Cordillera: Tectonics, v. 26, doi: 10.1029/2006TC001995.
- Mulch, A., Sarna-Wojcicki, A.M., Perkins, M.E., and Chamberlain, C.P., 2008, A Miocene to Pleistocene climate and elevation record of the Sierra Nevada (California): Proceedings of the National Academy of Science, v. 105, no. 19, p. 6819–6824.
- Noble, D.C., Slemmons, D.B., Korrington, M.K., Dickinson, W.R., Al-Rawi, Y., and McKee, E.H., 1974, Eureka Valley Tuff, east-central California and adjacent Nevada: Geology, v. 2, p. 139–142.
- Noble, D.C., Korrington, M.K., Church, S.E., Bowman, H.R., Silberman, M.L., and Heropoulos, C., 1976, Elemental and isotopic geochemistry of nonhydrated quartz latite glasses from the Eureka Valley Tuff, East-central California: Geological Society of America Bulletin, v. 87, p. 754–762.
- Oldow, J.S., 2000, Displacement transfer and differential block motion in the central Walker Lane, western Great Basin: Eos, Transactions, American Geophysical Union, v. 81, p. 1174.
- Pelletier, J.D., 2007, Numerical modeling of the Cenozoic geomorphic evolution of the southern Sierra Nevada, California: Earth and Planetary Science Letters, v. 259, p. 85–96.
- Pluhar, C.J., Deino, A.L., King, N.M., Busby, C., Hausback, B.P., Wright, T., and Fischer, C., 2009, Lithostratigraphy, magnetostratigraphy, and radio-isotopic dating of the Stanislaus Group, CA, and age of the Little Walker Caldera: International Geology Review, v. 51, doi: 10.1080/00206810902945017.
- Poage, M.A., and Chamberlain, C.P., 2002, Stable isotopic evidence for a pre-Middle Miocene rainshadow in the western Basin and Range: implications for the surface uplift of the Sierra Nevada: Tectonics, v. 21, p. 16-1–16-10.
- Priest, G.R., 1979, Geology and geochemistry of the Little Walker volcanic center, Mono County, California: Unpublished PhD thesis, Oregon State University.
- Proffett, J.M., 1977, Cenozoic geology of the Yerington district, Nevada, and implications for the nature and origin of Basin and Range faulting: Geological Society of America Bulletin, v. 88, p. 247–266.
- Putirka, K., and Busby, C.J., 2007, The tectonic significance of high K<sub>2</sub>O volcanism in the Sierra Nevada, California: Geology, v. 35, no. 10, p. 923–926.
- Ransome, F.L., 1898, Some lava flows on the western slope of the Sierra Nevada, California: United States Geological Survey Bulletin, v. 89, p. 71.
- Renne, P.R., Swisher, C.C., Deino, A.L., Karner, D.B., Owens, T., and DePaolo, D.J., 1998, Intercalibration of standards, absolute ages and uncertainties in <sup>40</sup>Ar/<sup>39</sup>Ar Dating: Chemical Geology (Isotope Geoscience Section), v. 145, p. 117–152.
- Repenning, C.A., 1960, Geologic summary of the central Valley of California with reference to the disposal of liquid radioactive waste: United States Geological Survey, Tace element Investigations Report 769, 69 pp.
- Roulet, F., 2006, The late Miocene Dixie Mountain Volcanic Center, Northern Sierra Nevada: eroded stratovolcano or laccolithic intrusion? [unpublished MS thesis]: University of California, Santa Barbara, 63 p.
- Saleeby, J., and Foster, Z., 2004, Topographic response to mantle lithosphere removal, southern Sierra Nevada region, California: Geology, v. 32, p. 245–248.
- Saleeby, J., Saleeby, Z., Nadin, E., and Maheo, G., 2009, Step-over in the structure controlling the regional west tilt of the Sierra Nevada microplate: eastern escarpment system to Kern Canyon system: International Geology Review, v. 51, p. 633–688.

- Saucedo, G.J., 2005, Geologic map of the Lake Tahoe basin, California and Nevada: Map no. 4, 1:100,000 Scale Regional Geologic Map Series, California Geological Survey.
- Saucedo, G.J., and Wagner, D.L., 1992, Geologic Map of the Chico Quadrangle, 1:250,000: California Division of Mines and Geology Regional Map Series, v. 7A.
- Schweickert, R.A., Lahren, M.M., Smith, K.D., and Karlin, R.D., 1999, Preliminary map of active faults of the Lake Tahoe basin: Seismological Research Letters, v. 70, p. 306–312.
- Schweickert, R.A., Lahren, M.M., Karlin, R.D., and Howle, J., 2000, Lake Tahoe active faults, landslides, and tsunamis, *in* Lageson, D.R., Peters, S.G., and Lahren, M.M., eds., Great Basin and Sierra Nevada: Boulder, Colorado, Geological Society of America Field Guide 2, p. 1–22.
- Schweickert, R.A., Lahren, M.M., Smith, K.D., Howle, J.F., and Ichinose, G., 2004, Transensional deformation in the Lake Tahoe region, California and Nevada, USA: Tectonophysics, v. 392, p. 303–323.
- Sella, G.F., Dixon, T.H., and Mao, A., 2002, REVEL: A model for recent plate velocities from space geodesy: Journal of Geophysical Research, v. 107, p. 1–17.
- Shuster, D.L., Flowers, R.M., and Farley, K.A., 2006, The influence of natural radiation damage on helium diffusion kinetics in apatite: Earth and Planetary Science Letters, v. 249, nos. 3–4, p. 148–161.
- Slemmons, D.B., 1953, Geology of the Sonora Pass region [PhD thesis]: Berkeley, University of California.
- Slemmons, D.B., 1966, Cenozoic volcanism of the central Sierra Nevada, California, Geology of Northern California: Bulletin of the California Division of Mines and Geology, p. 199–208.
- Smith, G.A., and Lowe, D.R., 1991, Lahars: Volcano-hydrologic events and deposition in the debris flow – hyperconcentrated flood flow continuum, *in* Fisher, R.V., and Smith, G.A., eds., Sedimentation in volcanic settings: SEMP Special Publication, v. 45, p. 59–70.
- Stewart, J.H., and Carlson, J.E., 1978, Geologic map of Nevada: U.S. Geological Survey in collaboration with Nevada Bureau of Mines and Geology, scale 1:500,000.
- Stock, G.M., Anderson, R.S., and Finkel, R.C., 2004, Pace of landscape evolution in the Sierra Nevada, California, revealed by cosmogenic dating of cave sediments: Geology, v. 32, p. 193–196.
- Stock, G.M., Anderson, R.S., and Finkel, R.C., 2005, Rates of erosion and topographic evolution of the Sierra Nevada, California, inferred from cosmogenic <sup>26</sup>Al and <sup>10</sup>Be concentrations: Earth Surface Processes Landforms, v. 30, p. 985–1006.
- Stockli, D.F., Surpluss, B.E., and Dumitru, T.A., 2002, Thermochronological constraints on the timing and magnitude of Miocene and Pliocene extension in the central Wassuk Range, western Nevada: Tectonics, v. 21, no. 4, p. 10-1–10-19.
- Surpluss, B.E., Stockli, D.F., Dumitru, T.A., and Miller, E.L., 2002, Two-phase westward encroachment of Basin and Range extension into the northern Sierra Nevada: Tectonics, v. 21, p. 1002.
- Thatcher, W., Foulger, G.R., Julian, B.R., Svarc, J.L., Quily, E., and Bawden, G.W., 1999, Present-day deformation across the Basin and Range Province, Western United States: Science, v. 283, p. 1714–1718.
- Unruh, J.R., 1991, The uplift of the Sierra Nevada and implications for late Cenozoic epeirogeny in the western Cordillera: Geological Society of America Bulletin, v. 103, p. 1395–1404.
- Unruh, J.R., Humphrey, J., and Barron, A., 2003, Transensional model for the Sierra Nevada frontal fault system, eastern California: Geology, v. 31, p. 327–330.
- Wagner, D.L., Jennings, C.W., Bedrossian, T.L., and Bortugno, E.J., 1981, Geologic map of the Sacramento quadrangle, California, 1:250,000: California Division of Mines and Geology, Regional Geologic Map 1A, scale 1:250,000.
- Wakabayashi, J., and Sawyer, T.L., 2001, Stream incision, tectonics, uplift, and evolution of topography of the Sierra Nevada, California: The Journal of Geology, v. 109, p. 539–562.
- Whitney, J.D., 1880, Harvard University, Museum of Comparative Zoology: Memoirs, v. 1, p. 659.
- Wolfe, J.A., Schorn, H.E., Forest, C.E., and Molnar, P., 1997, Paleobotanical evidence for high altitudes in Nevada during the Miocene: Science, v. 276, p. 1672–1675.
- Zandt, G., Gilbert, H., Owens, T., Ducea, M., Saleeby, J., and Jones, C., 2004, Active foundering of a continental arc root beneath the southern Sierra Nevada, California: Nature, v. 43, p. 41–45.